ABSTRACT

Kevin H. Dunn. An Investigation of Factors Affecting the Development of an Empirical-Conceptual Model for Estimating Spray Paint Exposure in a Cross Draft Spray Booth (Under the direction of Dr. Michael Flynn)

An empirical-conceptual modeling approach was developed by Carlton for estimating worker exposure to air contaminants during high pressure conventional air atomization spray painting. McKernan and Gatano sought to extend this model to the case of high volume, low pressure (HVLP) spray application technology. Significant differences between the Carlton and Gatano/McKernan model were established.

This research used a similar experimental methodology as Carlton and Gatano/McKernan to investigate the nature of these differences and to evaluate the sensitivity of the HVLP model to variations in test setup and sampling methodologies. A series of experiments using a mannequin, flat plate, and an HVLP spray application system were performed in a 25 ft^2 simulated cross draft spray booth. Spray gun hand orientation and lapel sampling location resulted in significant differences in measured breathing zone concentrations at similar test conditions. Minimal effects however were attributed to excessive wind tunnel blockage.

ACKNOWLEDGMENTS

I would like to thank my advisor, Dr. Michael Flynn for his guidance and support throughout this project. I would also like to thank my committee members Dr. Lori Todd and Dr. Michael Symons for their help in answering my questions and for helping to develop my skills under their instruction.

I would also like to thank my research partners John McKernan and Betty Gatano for working out the kinks in the system and providing me with a good base from which to start my studies. I would also like to acknowledge the efforts of Randall Goodman in setting up the paint booth for my use and providing materials and help in the second phase of testing. Finally, I would like to acknowledge the National Institute for Occupational Safety and Health (NIOSH) for providing funding for this research and financial support of my education. This work was supported by NIOSH grant #5 R01 OH02858, "Computational Methods in Industrial Ventilation."

TABLE OF CONTENTS

LIST OF TABLES

LIST OF FIGURES

1.0 Introduction

Spray finishing is a widely used process throughout industry for the coating of metallic parts, wood furniture, and even for the fabrication of fiberglass boats. A spray gun operates by atomizing liquid coatings with high pressure air (conventional spray guns) or through a high volume of low pressure air (HVLP spray guns). The droplets formed from this process are propelled towards the workpiece with some impacting on the part. A significant portion of the liquid however does not coat the part and is carried away by the air stream, sometimes reaching the breathing zone of the worker. The inhalation of these small droplets, called overspray, may result in adverse health effects for the worker. [1] Paints consist of several chemical components including inorganic pigments diluted in a mixture of solvent carrier, binder, and other additives to enhance coating properties. Common pigments used in paints contain compounds of toxic metals including lead, cadmium, and chromium. Another hazardous component used primarily in automotive clear coats is isocyanates which have resulted in skin and eye irritation as well as respiratory effects.[1,2]

The primary exposure control method used in the spray painting of large parts is a ventilated booth. The conventional spray booth is constructed of sheet metal with an open entrance for conveying parts into and out of the paint area. An exhaust fan in the rear of the booth typically delivers air velocities of around 100 feet per minute (fpm) to control

solvent buildup (flammability), to prevent contamination of the part coating and to minimize worker exposure to toxic chemicals.[3] Recently, a new generation of high transfer efficiency application devices have been studied to evaluate their impact on reducing air emissions of process contaminants and subsequently worker exposure to these chemicals. The transfer efficiency is the ratio of the amount of material sprayed to the amount of material deposited on the workpiece. A high transfer efficiency means that more material is transferred to the part and less material is exhausted from the process.

The effect of higher transfer efficiency may translate into reduced worker exposure to overspray contaminants. A comparison of conventional and HVLP spray guns conducted by the National Institute of Occupational Safety and Health (NIOSH) showed that the HVLP system tested was about 30% more efficient than the conventional spray gun based on measured film thickness. The corresponding particulate overspray concentration was reduced by a factor of 2. A theoretical derivation of the relationship between transfer efficiency and air contaminant concentration shows that increased transfer efficiencies result in a greater than proportional decrease in solvent and particulate overspray concentration.[4] Recent recommendations by NIOSH based on these results have placed emphasis on the use of HVLP as a mechanism to minimize overspray generation. NIOSH released a Hazard Controls Bulletin in January 1996 which recommended the use of HVLP, downdraft ventilation and respiratory protection to control worker exposure to toxic contaminants.[5]

Most companies are slowly replacing their conventional spray guns with the newer HVLP systems. The reasons for these conversions are two-fold: changing environmental regulations and reducing operating costs. In 1989, the South Coast Air Quality Management District (SCAQMD) became the first region of the country to mandate the use of HVLP or other high transfer efficiency coating technologies (transfer efficiency greater than 65%).[6] The SCAQMD has gone on to mandate the use of high transfer efficiency application technologies in several other sectors including automotive body shops (Rule 1151), fiberglass fabrication (Rule 1162) and wood furniture manufacturing (Rule 1136). [7,8,9] The Environmental Protection Agency (EPA) has followed suit in its development of the National Emissions Standards for Hazardous Air Pollutants (NESHAP). The recently promulgated Wood Furniture Maximum Achievable Control Technology (MACT) standard restricts the use of conventional spray guns in most application processes used in furniture manufacturing.[10]

1.1 Background and Objectives

One of the primary goals of local exhaust ventilation and the use of the new high transfer efficiency spraying equipment is to limit worker exposure to air contaminants to an acceptable level. Although the American Conference of Governmental Industrial Hygienists (ACGIH) ventilation design manual provides recommendations on paint booth design and operational parameters (like air flow rate) [3], the ability of these engineering controls to meet the recommended limits is not known until personal sampling is

performed. Carlton developed an empirical-conceptual model to relate worker exposure to spray painting process parameters. [11] This conceptual model attempted to account for the main processes which lead to worker exposure. The resulting model defined worker exposure in terms of seven major factors including: overspray mass generation rate (m_0) ; spray nozzle pressure (p_n); paint viscosity (μ_l); freestream velocity (U); dimensions of the worker (height, H and breadth, D); and worker orientation to the freestream (see Figure 1). Based on each of the primary processes, the relevant parameters were chosen and grouped into two dimensionless ratios which incorporated aspects of each important exposure mechanism. The following are the non-dimensional groupings:

Carlton number (non-dimensional nozzle pressure): $\frac{p_n H}{\mu_l U}$

Non-dimensional Concentration: $\frac{CHUD}{m_0}$

A mannequin, flat plate, and conventional pneumatic spray atomization nozzle were used in a small scale wind tunnel to evaluate the functional relationship between these two groups. Carlton performed a series of tests with the mannequin and workpiece oriented in both the 180^0 (airflow is to the worker's back) and 90^0 (airflow is to the worker's side) to develop the model for each of these commonly used configurations (Figure 1). A regression of the data set gathered by Carlton resulted in the following relationships. [11]

90^0 orientation:

$$\frac{CHUD}{m_0} = \frac{1}{\left\{7.44 + 1.08x10^3 \exp\left[-5.64x10^{-7}\frac{p_n H}{\mu_l U}\right]\right\}}, \qquad r^2 = 0.98$$

180^0 orientation:

$$\frac{CHUD}{m_0} = 3.23x10^{-2} \exp\left[-1.94x10^{-7}\left(\frac{p_n H}{\mu_l U}\right)\right], \quad \text{for } \frac{p_n H}{\mu_l U} < 10^7, \; r^2 = 0.95$$

$$\frac{CHUD}{m_0} = 0.006, \quad \text{for } \frac{p_n H}{\mu_l U} > 10^7$$

Further research performed by Gatano and McKernan sought to extend this model to a High-Volume, Low-Pressure spray gun.[12] A similar experimental methodology was employed including: a full scale automated mannequin, a larger flat plate and a commercial HVLP spray gun system installed in the small experimental wind tunnel. The results of their research showed a significant difference in the 90^0 orientation from the Carlton model. A plot of the results of both the Gatano/McKernan and Carlton data set is shown in Figure 2.[11,12]

This study sought to evaluate the nature of the differences between the Carlton model and the Gatano/McKernan HVLP results. The sensitivity of the HVLP model to various operational and sampling alternatives was investigated to determine if differences in the experimental methodologies used by McKernan and Gatano could account for the variation between their results and the Carlton model. The effects of three setup configurations on the model were evaluated in this study including: spray gun hand orientation (see Figure 3); concentration sample location (upstream versus downstream lapel); and wind tunnel blockage ratios. These effects were evaluated only in the 90^0 orientation as the McKernan/Gatano data set fit the Carlton model well in the 180^0 orientation.

The difference between handedness was investigated for the 90^0 worker orientation. The mannequin throughout this experimental study had the spray gun placed in the upstream hand (see Figure 3). A series of tests were performed by Gatano and McKernan with the gun in the downstream hand of the mannequin. A comparison of the differences between the non-dimensional concentration across a range of Carlton numbers was examined to determine the impact of handedness on the model development for the HVLP system. The effect of sample location was also investigated during this study. The mannequin was outfitted simultaneously with a sampler on both the upstream and downstream lapel. The resulting concentrations were analyzed to determine if a sampling location choice resulted in a significant difference in measured breathing zone concentrations. The final research question which was investigated during this study was

the effect of scaling or tunnel blockage ratios. The blockage ratio is the ratio of the area of the test object (mannequin and plate) to the cross-sectional area of the overall test section (wind tunnel). To investigate the magnitude of these effects, the mannequin and spray system were moved from the small scale experimental wind tunnel into a full size paint booth and a series of test conditions were run.

2.0 Conceptual Model Development Theory

The benefit of the empirical-conceptual modeling approach is that once a limited number of process parameters are known, an estimate of worker exposure can be calculated. Also, the benefits of altering some of these parameters, such as increasing spray booth exhaust flow rates, can be semi-quantitatively evaluated. This modeling approach was employed by Carlton for the conventional spray system and focused on evaluating the parameters of the three main processes which lead to worker exposure to hazardous contaminants.[11]

The main processes which dominate exposure in spray painting tasks include paint droplet formation, transfer, and overspray transport.[11] The spray gun produces droplets by the shear forces generated by the action of the high velocity gas acting on the liquid jet. The atomization air is delivered in a parallel flow pattern around the liquid. The HVLP spray gun has a pair of air atomization orifices which surround the liquid orifice and delivers a high volume of low pressure air to cause the liquid stream to disintegrate into a

fine spray mist. This process is called pneumatic atomization and is used in spray painting to produce droplets typically less than 50 μm in size which are in turn deposited on the workpiece by impaction.[13]

Droplet formation is the first stage of the process which leads to paint deposition and the generation of overspray. The droplet size distribution generated by pneumatic aspiration has been shown to be a function of the mass flow rates of air and liquid, the physical properties of the fluid, and the relative velocity of the liquid to the gas stream. Kim and Marshall developed an empirical relationship for determining the mass median diameter of droplets produced by atomization and reported these findings [13]:

1) The mass median diameter of a spray decreased to a limiting mass median diameter as the ratio of the mass flow rates of air to liquid (m_a/m_l) increases;

2) An increase in liquid viscosity (μ_l) results in an increase in the mass median diameter of the droplets produced by atomization; and

3) The mass median diameter of a spray at a constant m_a/m_l was larger for lower air velocities for a given atomizer.

A conventional spray gun atomizes at a higher nozzle pressure than an HVLP system (65 psi vs. 10 psi). This higher pressure results in a relative velocity between the

spray droplets and the atomization air stream being much higher for the conventional system than the HVLP spray gun. The conventional spray system however operates at a lower m_a/m_l than the HVLP gun since the volumetric flow rate of atomization air for a conventional gun is significantly lower than that of the HVLP. These operational differences result in the spray distribution (MMD) generated by the HVLP being larger than that produced by a conventional spray gun. The larger droplets produced result in differences in both droplet transfer characteristics and solvent evaporation rates because of the lower total surface area of the HVLP distribution than the finer droplet distribution produced by the conventional spray gun.

The spray droplet transfer process is another major component in the determination of worker exposure. After the droplets leave the gun, they are propelled by the momentum imparted to them by the jet and the surrounding envelope of atomization air. As the jet meets the workpiece, the flow is diverted along the boundary of the flat plate. Some of the larger particles with sufficient inertia will impact on the plate while the smaller particles will be carried along the stream lines away from the workpiece. Simple impaction theory indicates that the cut size (size at which 50% of the particles of a given size will impact the plate) of the impaction process is proportional to the particle size. Therefore, larger particles will most likely be transferred to the workpiece while the smaller particles will be conveyed away from the workpiece by the freestream. As was previously shown, the HVLP produces a coarser spray droplet distribution and therefore more droplets are likely to impact resulting in a higher transfer efficiency and a lower

contaminant overspray generation rate than the conventional spray system. This result has been shown in practice with conventional spray transfer efficiencies typically ranging from 30-40% while HVLP transfer efficiencies have been reported above 65%.[4] Another difference in the droplet transport mechanisms of the HVLP and the conventional atomizer used by Carlton is the substantially higher momentum flux of the HVLP spray gun due to its higher volumetric air flow rate. The parameter used in the model to account for droplet transfer mechanisms is the nozzle pressure (p_n).

The final process considered in the model development is overspray transport. The overspray is the collection of particles which do not have the inertia required to deviate from the air stream and impact on the part. Researchers have shown that these particles are generally 2.9-9.7 μm in size.[14] These droplets are diverted along the workpiece boundary and dispersed by the action of the jet and the booth freestream. The spray booth ventilation system is designed to transport these droplets away from the part and collect them by dry filtration or by wet scrubbers.

The research performed by Carlton showed a significant difference in overspray exposure based on the worker/workpiece orientation.[11] The traditional recommended orientation is to place the contaminant generation source (spray gun) between the worker and the exhaust. George et al. showed that a reverse flow region formed downstream of the worker due to vortex shedding.[15] This reverse flow region caused contaminants to be transported back into the workers breathing zone. The breathing zone concentration

(BZC) was shown to be a function of the freestream velocity (U), the worker's height (H) and the worker's breadth (D) by George et al. and other researchers.[15,16,17] The George et al. study, however, was performed with a source of negligible momentum and did not simulate a realistic spray painting operation. Kim and Flynn subsequently showed that the addition of a strong contaminant injection rate, similar to the case for spray painting, eventually prevents the formation of this vortex street and resulted in a dramatic reduction in the BZC of contaminants when compared to the case with a quiescent source.[18]

3.0 Experimental Methodology

The experimental setup shown in Figure 4 was used to determine the relationship between the non-dimensional groupings of interest. A mannequin was placed in a wind tunnel which simulated a cross draft spray paint booth. The mannequin was outfitted with an electronically controlled trigger device which allowed for remote activation/deactivation of the spray painting gun. A 3 x 3 foot flat plate was used to simulate a workpiece. The use of a flat plate was chosen to enhance reproducibility among runs due to uniform air jet rebound characteristics. The mannequin was also outfitted with an air sampling cassette to measure breathing zone concentrations. The runs were performed with the mannequin oriented 90^0 to the freestream (see Figure 1). The spray gun was held in the upstream hand for comparison with additional data to evaluate the impact of handedness on breathing zone concentration. Breathing zone

samples were taken on both the upstream and downstream lapel to determine the effect of sampling location on measured concentration.

The wind tunnel has a cross sectional area of 25 ft^2 (5 ft by 5 ft) and is eight feet in depth. A bell-shaped inlet flange was constructed on the entry to reduce the effects of flow separation and to provide a more uniform flow. A pegboard and filter bank were also installed in the rear of the tunnel to assist in maintaining uniform flow throughout the depth of the tunnel. A pitot tube was installed to provide an indication of the tunnel static pressure and an air flow calibration curve was generated by performing a 16 point hot wire anemometer traverse across the tunnel cross sectional area. Tunnel freestream velocities of 45-325 feet per minute (fpm) were measured at tunnel static pressures ranging from 0.02 to 0.7 inches of water. Average freestream velocities from 75-350 fpm with longitudinal component of freestream turbulence intensities of 6-11% are possible in the tunnel.[11]

Following the completion of the experimental runs in the wind tunnel, the test setup including the mannequin and HVLP spray system was relocated to a full size paint booth located on the campus of the University of North Carolina at Chapel Hill. The paint booth cross sectional measurements were 7.25 ft x 6.25 ft and was 13.5 ft in depth. The room housing the paint spray booth was in the machine shop of the School of Public Health with several benches and cabinets located near the inlet to the booth which caused fairly high turbulence in the paint booth. A sheet metal flange was also installed on the

entrance to the booth to minimize the effects of flow separation at the booth entrance. The flowrate through the tunnel is adjustable by varying a pulley on the fan belts which in turn controls the fan speed. The fan was set initially to provide approximately 100 fpm and was not varied during the experiment due to difficulty in precise adjustment of fan speed. The air velocity was measured by the thermo-anemometer on a 12 point grid across a the paint booth cross section. A series of experiments were run in the paint booth to evaluate the effects of wind tunnel blockage on the exposure model.

The test system used was a pressure fed HVLP spray painting system (see Figure 5). A compressor was set to 100 psi to provide a constant source of air to the feed tank. The compressor also had a filter on the outlet to remove any moisture, dusts, or oils from the feed air. The air pressure was regulated at the feed tank to maintain approximately 10 psi on the liquid feed while the pressure to the gun was regulated separately to attain the desired air cap pressure for testing.

A DeVilbiss MSV-533-4-FF model HVLP spray gun was used throughout the test. The spray gun is constructed out of 400 grade stainless steel and fitted with a #33A air cap which is recommended for most common coating materials with required flow rates up to 12 oz/min. The spray gun is designed to operate at a nominal air cap pressure of 10 psi. The gun will produce 10 psi at the cap when the gun inlet pressure is set to a nominal pressure of 50 psi. An air cap test kit was used to measure the pressure at the cap while varying the gun inlet pressure at the feed tank regulator. The gun is also outfitted with 2

knobs to allow the operator to easily adjust the flow of air or liquid. The operator typically will make adjustments to the liquid flowrate based on the required coating thickness. Adjustment of the air knob allows the operator to control the fan pattern produced by the gun. This control knob would be adjusted based on the shape and size of the workpiece.[19] The air knob was set to produce an elliptical pattern used frequently in manufacturing. The liquid and air knobs were not adjusted throughout testing so that good reproduction of test conditions could be achieved from run to run.

Inland #99 neutral parrafinic vacuum pump oil was used instead of actual paint during this experiment. This was done mostly due to safety concerns with using paint. The vacuum pump oil was selected based on nonvolatility and because its viscosity is similar to enamel paints. The oil is also compatible with the materials in the wetted sections of the spray gun. The variation of the viscosity with temperature was measured using a Haake falling ball viscometer and corrections were applied to the data to account for actual environmental conditions.

Determination of Overspray and Transfer Efficiency

The calculation of overspray generation rate and transfer efficiency was performed based on mass balance methodology. The amount of liquid sprayed was calculated by weighing the feed pot before and after each experimental run. The liquid mass flowrate was calculated by dividing the mass of the liquid sprayed by the run time. A trough was

placed under the flat plate to collect all the spray droplets that had impacted on the part. This trough was weighed before and after each run to measure the amount of liquid transferred to the workpiece. A simple ratio of the amount of the liquid transferred to the workpiece to the total amount of liquid used during the run provided the transfer efficiency. The mass overspray generation rate (m_0) was also calculated by subtracting the mass flow rate of liquid transferred to the workpiece from the total mass flow rate of liquid used during each run.

Determination of Breathing Zone Concentration

NIOSH Method 0500 for total aerosol mass was used to perform the sampling and analysis of all breathing zone concentrations (C). A 37 mm polyvinyl chloride filter with a 5 μm pore size was used at a sampling rate of 2.0 lpm.[20] An Aircheck personal sampling pump Model No.224-PCXR8 was used throughout the test. Run time was adjusted to collect an adequate sample mass (0.1-2 mg) for weighing and typically ranged from 5-10 minutes. Filter weights were measured by a Cahn 27 electrobalance which has a sensitivity of 0.0001 mg and a stated accuracy of ± 0.005%.

Previous research has shown that open and closed faced cassettes tend to significantly under-represent the aerosol when sampling from a moving airstream with the sampler oriented normal to the airstream (as in this research).[21] A sampler developed by the Institute of Occupational Medicine (IOM) was used in this study to minimize the

effects of under-sampling associated with the open and closed face cassettes. Mark and Vincent developed the British personal inhalable aerosol sampler (PIAS) which is comprised of a 37 mm cassette with a circular 15 mm diameter entry.[22] A test performed by the IOM evaluated many different international personal samplers by placing the sampler on a mannequin and rotating the mannequin through 360^0 during each run to achieve a non-orientation specific sample. The IOM testing was performed over a range of freestream velocities from 0.5-3.0 m/s and a range of particle sizes up to about 75 μm. The PIAS showed sampling efficiencies which were consistent with the ACGIH Inspirable Particulate Mass (IPM) curve which represents what a worker breathes in through the nose and mouth during normal respiration. The gravimetric analysis method recommended by the IOM was to weigh the complete cassette before and after each run to minimize particle losses to the internal surfaces of the sampler.[23] These losses have been shown to be a significant portion of the overall mass aspirated by the sampler (up to 40%).[24] In accordance with NIOSH method 0500, only the filter was weighed before and after the runs therefore, the results of the samples in this study are therefore likely to be less than the actual concentration of contaminant in the breathing zone.

4.0 Results

4.1 Differences between Upstream and Downstream Hands

During this research, runs were performed with the spray gun in the upstream hand for comparison with the Gatano/McKernan downstream hand data set. Breathing zone concentrations were taken on the downstream lapel for all of the Gatano/McKernan data set. Only the downstream lapel samples from the upstream hand data set are therefore used for comparison to the Gatano/McKernan data set to minimize any bias introduced by the choice of sample location. A linear plot of the Carlton number versus the non-dimensional concentration is shown for both upstream and downstream hand orientations (see Figure 6). This plot shows that the upstream hand non-dimensional concentrations are much lower than the downstream hand concentration at Carlton numbers greater than 1.0×10^6. Also, a difference in transfer efficiency between the two data sets (upstream and downstream hand) was observed. The plot of transfer efficiency versus the ratio of mass flow rate of air to liquid is shown in Figure 7. The transfer efficiency measured during the upstream hand runs was noticeably higher than the downstream runs from the Gatano and McKernan data set.

4.2 Sample Location Effects

The mannequin was outfitted with air sampling cassettes on both the upstream and downstream lapel during the experimental wind tunnel test runs. The effects of sample location on the measured breathing zone concentration (BZC) are shown in Table 1. As can be seen, for all cases in the 90^0 orientation with the gun in the upstream hand, the contaminant concentration measured on the downstream lapel was consistently higher than that of the upstream lapel. The downstream concentration was were primarily between 5-30% (7 of 11) percent higher than the corresponding upstream lapel measured concentrations.

4.3 Tunnel Blockage Ratios and Scaling Effects

To investigate the effects of wind tunnel blockage on the model, the mannequin and flat plate were moved from the small experimental wind tunnel into a larger full size spray booth. The paint booth freestream velocity was set to a nominal value of approximately 100 fpm and the HVLP nozzle pressure was varied to map out a region of Carlton numbers. The results of the runs performed in the paint booth are shown along with the results of the wind tunnel data in Figure 8. The least squares regression line for the wind tunnel data is plotted to illustrate the distribution of the paint booth data with respect to the wind tunnel data. As seen in the figure, the paint booth non-dimensional concentrations seem to be consistent with the wind tunnel data at high Carlton numbers but are slightly lower than the wind tunnel data at lower Carlton numbers.

5.0 Discussion

5.1 Differences between Upstream and Downstream Handedness

The differences in handedness are believed to be due to the impact of the differences in the flow patterns of the overspray mist. As can be seen in Figure 9, if the spray gun is moved from the upstream to the downstream hand, the cloud generated by the overspray mist (jet 1) would be translated towards the breathing zone of the worker. As the spray gun is moved to the downstream hand, the contaminant cloud recirculation zone is moved towards the breathing zone (and the downstream lapel) of the worker. As the overspray mist is formed from the spraying operation (when the gun is in the upstream hand), the droplets have a longer length to travel to reach the breathing zone of the worker. This allows the droplets to be dispersed by the fresh air entering the booth and results in lower breathing zone concentrations. The BZCs measured during the downstream hand spraying were approximately 2-7 times greater than those measured during upstream hand spraying. The mannequin arm was stationary during both the upstream and downstream testing, however, an additional study incorporating side to side motion was performed with the gun in the downstream hand (see Figure 10). The results showed that contaminant concentrations were significantly reduced possibly indicating an averaging of the upstream and downstream hand effects.

The handedness differences seen also hint at a difference in contaminant concentration regimes. As can be seen from Figure 6, there is a linear relationship

between non-dimensional nozzle pressure and BZC for the upstream hand orientation. This implies that as the Carlton number increases (indicating an increase in nozzle pressure and/or a decrease in the wind tunnel freestream velocity) the contaminant concentration linearly increases. This outcome makes intuitive sense with the factors discussed thus far. If the paint booth velocity is increased, we'd expect to see a decrease in the BZC. Also, as discussed previously, as the nozzle pressure is increased, the transfer efficiency decreases and the BZC also increases. There is a practical limit however where an increase in nozzle pressure will no longer result in an increase in worker BZC. This is due to the fact that at some limiting nozzle pressure, the region around the worker begins to resemble a well mixed volume. In this operational regime, the rate of overspray entering the worker's breathing zone equals the rate of overspray removed by the exhaust flow. This operational condition was reached during the downstream hand spray tests at a non-dimensional nozzle pressure of approximately greater than 1.0E+06. The upstream hand testing showed that this point was not reached even at Carlton numbers of approximately 2.3E+06. This may be indicative of the differences in the overspray plume between each of these orientations.

The differences in the transfer efficiency seen in Figure 7 are puzzling. The wind tunnel and paint booth results of the upstream hand transfer efficiencies were consistently higher than those of the downstream hand. The paint booth data, however, was closer to the downstream hand data set. The most logical reason for a difference would seem to be a difference in test set up or conduct. The lower transfer efficiencies seen in the

McKernan/Gatano data set might be due to the placement of the workpiece with respect to the spray gun. The flat plate position may affect the transfer efficiency by altering the amount of overspray which is diverted behind the workpiece. The plate was centered on the spray gun from side to side for the upstream hand data sets. The spray gun distance was set and checked prior to each run and was held at a eight inches from the plate and is not suspected to have caused the discrepancies.

5.2 Sample Location Effects

A Wilcoxon signed rank test was performed to validate the observed differences seen in Table 1. The test showed a difference at a level of significance of $p < 0.01$. The greatest differences were observed at low nozzle pressures corresponding to the lowest sample masses which would have inherent variance. The reason for the differences may be due to the effects of the wake of the gun discharge. As the spray gun propels the paint towards the workpiece, one jet of material flows toward the tunnel exhaust while a second jet is directed towards the booth inlet (see Figure 9). NIOSH showed that the second jet is dispersed into the oncoming air stream and flows back into the worker's breathing zone.[1] Both lapel samples will therefore receive the majority of the sampled mass from the second jet stream. However, the downstream lapel may also receive a dose from the first jet due to the reverse flow region formed downstream of the body whereas the upstream lapel is unlikely to receive a significant dose from the first jet. This phenomenon may be unique to the upstream hand configuration as the effect should be

diluted as the downstream jet is moved closer to the exhaust filters (i.e. to the downstream hand).

5.3 Tunnel Blockage Ratios and Scaling Effects

Previous researchers have shown that the flow characteristics change depending on the overall blockage of the test section. Taylor and Whitelaw observed that as the blockage ratio increased, there was an increase in the length and a decrease in the width of the recirculation region downstream of the test object.[25] The consequences of these effects with respect to the test situation of placing a near full size mannequin and plate in a small experimental wind tunnel were unknown. The blockage ratio of the paint booth and wind tunnel are shown in Table 2 for comparison. The regression line for the analogous wind tunnel data is plotted along with the results of the paint booth data are shown in Figure 8. As one can see, the effects of blockage seem to create minimal effects. At higher non-dimensional nozzle pressures, the data points lie distributed about the wind tunnel regression line. However, at low nozzle pressures, the concentrations were slightly lower than those measured in the wind tunnel. A partial F test was performed to determine if the slopes and intercepts of the regressions were equal.[26] The result of the F test indicated that the lines were coincident at a level of significance of 0.05. Therefore in the nominal operational region of the HVLP system, the wind tunnel blockage did not seem to have caused a significant bias in the data set. This effect however, may be

important in the 180^0 orientation as the blockage ratio is substantially higher than that of the 90^0 orientation.

6.0 Conclusions

A significant difference exists between the model developed by Carlton for the conventional spray gun and the HVLP system for the 90^0 orientation. These differences can be seen in Figure 11. The results of the Carlton model showed that the relationship between the non-dimensional groups is fairly constant within the region of operation for conventional spray guns (Carlton numbers of 1.2×10^7 to 2.0×10^7) with $CHUD/m_0$ values for the 90^0 orientation greater than an order of magnitude higher than the 180^0 orientation. However, these curves show a crossover at lower values of the Carlton number (less than 5.0×10^6) suggesting that the 90^0 orientation might be preferable when operating in this region, as with the HVLP system.[11] The results of the research performed by McKernan and Gatano as well as the tests performed by the author of this paper suggest that this is not the case. Although the McKernan/Gatano 180^0 orientation HVLP data seems to match up with the Carlton model, the 90^0 orientation results suggest that a mechanism not considered in the Carlton model may be resulting in significantly higher non-dimensional concentrations than predicted.[12]

There is also a significant difference between the exposures measured associated with the hand position of the spray gun. The downstream hand resulted in a measured

breathing zone concentration that was a factor of 2-7 times higher than that of the upstream hand. This effect is diluted however when a side to side motion was tested. This result suggests that testing of actual spray painting operations needs to be completed before a thorough evaluation of this model can be completed. In many cases, work practices will result in significant variability between this model and actual measured concentrations. Therefore, this model may be useful in that it may provide an order of magnitude estimate of exposure and may help in evaluating optimizing process parameters to reduce worker exposure.

The effects of sampling location and tunnel blockage ratios were also studied. The comparison of lapel sampling locations showed higher breathing zone concentrations measured consistently on the downstream lapel. This result suggests that the conservative approach to evaluating worker exposure to contaminants, in the 90^0 orientation with the spray gun in the upstream hand performed in a cross draft booth, would be to place the sampler on the downstream lapel of the worker. The lapel samples should tend to give a higher concentration than the actual breathing zone because of the effects of the reverse flow region which occur downstream of the body. Finally, the wind tunnel blockage ratio did not seem to significantly affect the results of the experiments. The results of the full scale paint booth test runs showed that at moderate Carlton numbers, there were negligible differences in the non-dimensional concentration number while at low pressures the non-dimensional concentrations were slightly lower than those measured in the wind tunnel.

REFERENCES

1. Heitbrink, W.A.; Wallace, M.E.; Bryant, C.J.; Ruch, W.E.: Control of Paint Overspray in Autobody Repair Shops. **Am. Ind. Hyg. Assoc. J.** 56:1023-1032 (1995).

2. Burgess, W. A.: Recognition of Health Hazards in Industry, A Review of Materials and Processes, pp. 247-275. John Wiley and Sons, Inc., New York, NY (1995).

3. American Conference of Governmental Industrial Hygienists: Industrial Ventilation, A Manual of Recommended Practice. ACGIH, Cincinnati, OH (1995).

4. Heitbrink, W.A.; Verb, R.H.; Fischbach, T.J.; Wallace, M.E.: A Comparison of Conventional and High Volume-Low Pressure Spray-Painting Guns. **Am. Ind. Hyg. Assoc. J.** 57:304-310 (1996).

5. National Institute for Occupational Safety and Health: Control of Paint Overspray in Autobody Repair Shops. DHHS (NIOSH) Publication No. 96-106. NIOSH, Cincinnati, OH (1996).

6. Cedoz, R.; Treuschel, J.: HVLP, the 'Wonder' Gun. **Industrial Finishing**. (1993).

7. South Coast Air Quality Management District: "Regulation XI source specific standards, Rule 1151, Motor Vehicle and Mobile Equipment Non-Assembly Line Coating Operations" (amended March 8, 1996), South Coast Air Quality Management District, Diamond Bar, CA (local air pollution control regulation).

8. South Coast Air Quality Management District: "Regulation XI source specific standards, Rule 1162, Polyester Resin Operations" (amended May 13, 1994), South Coast Air Quality Management District, Diamond Bar, CA (local air pollution control regulation).

9. South Coast Air Quality Management District: "Regulation XI source specific standards, Rule 1136, Wood Products Coatings" (amended June 14, 1996), South Coast Air Quality Management District, Diamond Bar, CA (local air pollution control regulation).

10. U.S. Environmental Protection Agency: "Final Standards for Hazardous Air Pollutant Emissions from Wood Furniture Manufacturing Operations; Final Rule", 40 CFR Parts 9 and 63 (1995).

11.Carlton, G.N.: A Model to Estimate Worker Exposure to Spray Paint Mists. Ph.D. Thesis, University of North Carolina at Chapel Hill, NC (1996).

12. McKernan, J.: Effect of position and Motion on Personal Exposure in a HVLP Spray Painting Operation. Masters Technical Report, University of North Carolina at Chapel Hill, NC. (1997).

13. Kim, K.Y.; Marshall, W.R.: Drop-Size Distributions from Pneumatic Atomizers. **AIChE J.** 17(3):575-584 (1971).

14. D'Arcy, J.B.; Chan, T.L.: Chemical Distribution in High Solids Paint Overspray Aerosols. **Am Ind. Hyg. Assoc. J**. 51(3):132-138 (1990).

15. George, D.K.; Flynn, M.R.; Goodman, R.: The Impact of Boundary Layer Separation on Local Exhaust Design and Worker Exposure. **Appl. Occup. Environ. Hyg.** 5(8): 501-509 (1990).

16. Kim, T.; Flynn, M.R.: Modeling a Worker's Exposure From a Hand-Held Source in a Uniform Freestream. **Am. Ind. Hyg. Assoc. J.** 52(11):456-463 (1991).

17. Kim, T.; Flynn, M.R.: Airflow Pattern Around a Worker in a Uniform Freestream. **Am. Ind. Hyg. Assoc. J.** 52(7):287-296 (1991).

18. Kim, T.; Flynn, M.R.: The Effect of Contaminant Source Momentum on a Worker's Breathing Zone Concentration in a Uniform Freestream. **Am. Ind. Hyg. Assoc. J.** 53(12): 757-766 (1992).

19. DeVilbiss: The ABC's of Spray Finishing, A Working Guide to the Selection and Use of Spray Finishing Equipment. ITT DeVilbiss Maumee, OH (1995).

20. National Institute for Occupational Safety and Health: Particulates Not Otherwise Regulated, Total: Method 0500. In: NIOSH Manual of Analytical Methods, 4th Edition. P.M. Eller, Ed. NIOSH, Cincinnati, OH (1994).

21. Buchan, R.M.; Soderholm, S.C.; Tillery, M.I.: Aerosol Sampling Efficiency of 37 mm Filter Cassettes. **Am. Ind. Hyg. Assoc. J.** 47(12):825-831 (1986).

22. Mark, D.; Vincent, J.H.: A New Personal Sampler for Airborne Total Dust in Workplaces. **Ann. Occup. Hyg.** 30(1):89-102 (1986).

23. Vincent, J.H.; Mark, D.: Entry Characteristics of Practical Workplace Aerosol Samplers in Relation to the ISO Recommendations. **Ann. Occup. Hyg.** 34(3): 249-262 (1990).

24. Demange, J.; Gendre, J.C.; Herve-Bazin, B.; Carton, B.; Peltier A.: Aerosol Evaluation Difficulties Due to Particle Deposition on Filter Holder Inner Walls. **Ann. Occup. Hyg.** 34(4): 399-403 (1990).

25. Taylor, A.M.K.P.; Whitelaw, J.H.: Velocity Characteristics in the Turbulent Near Wakes of Confined Axisymmetric Bluff Bodies. **J. Fluid Mech.** 139:391-416 (1984).

26. Kleinbaum, D.G.; Kupper, L.L.; Muller, K.E.: Applied Regression Analysis and Other Multivariate Methods, pp. 271-274. 2nd ed. Duxbury Press, Belmont, CA (1988).

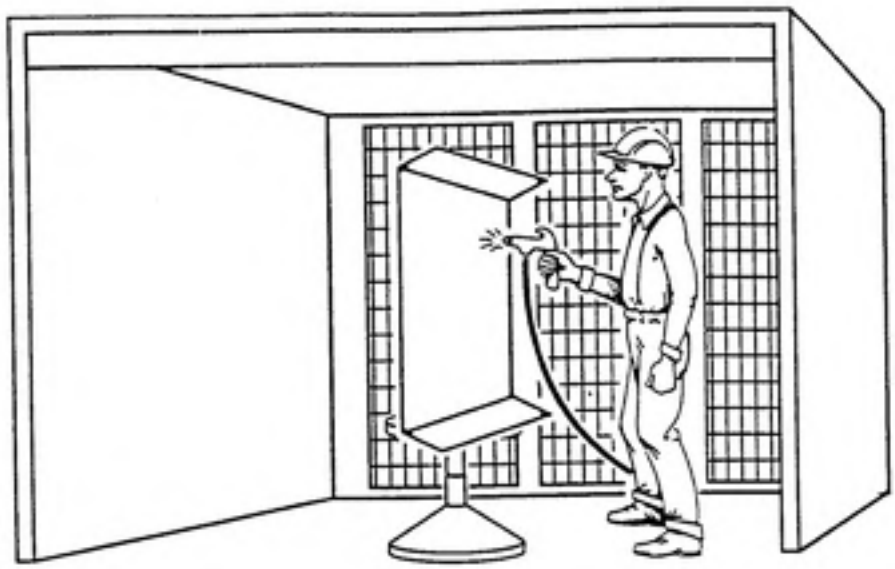

90° Orientation

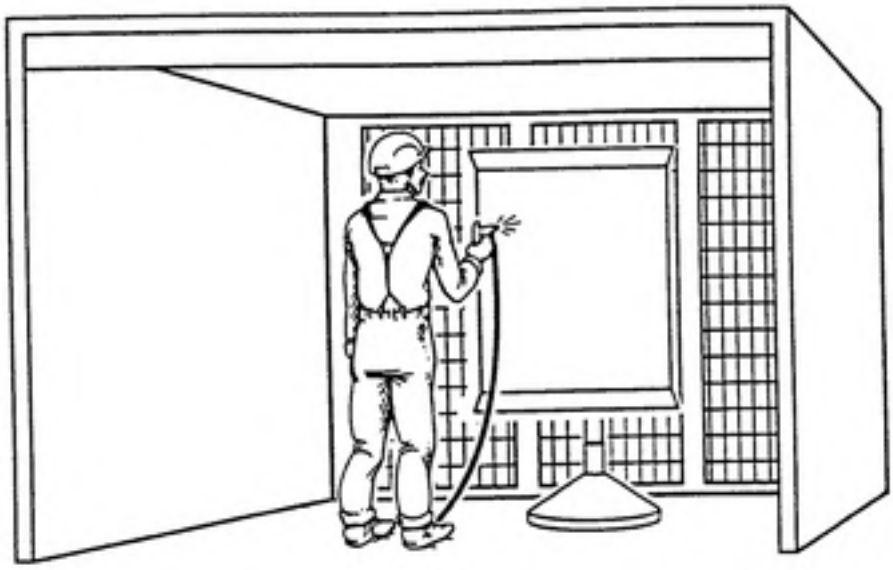

180° Orientation

Figure 1: Spray Painting Worker/Workpiece Orientation

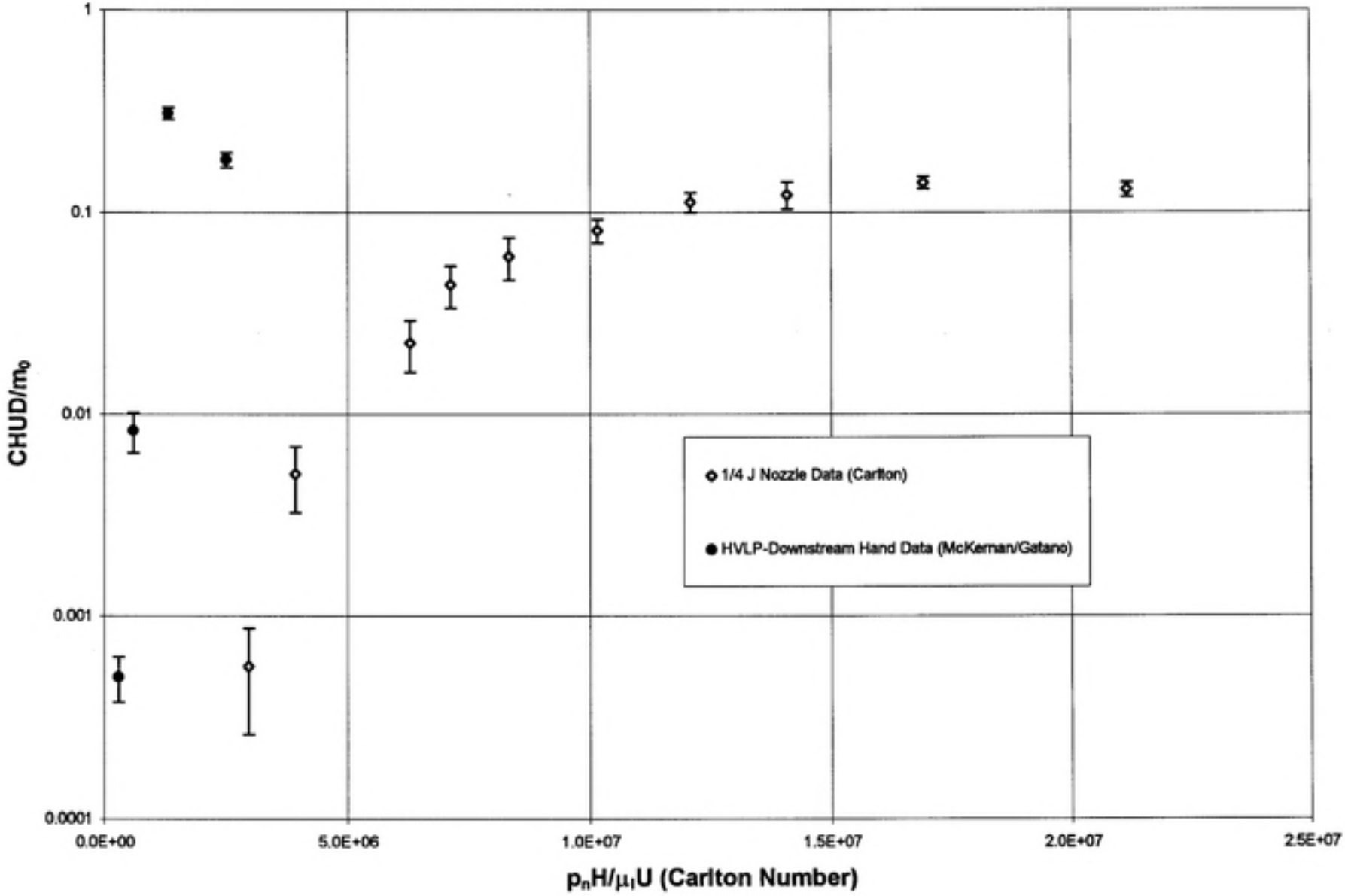

Figure 2: Functional relationship between the dimensionless groups for Carlton and McKernan/Gatano datasets

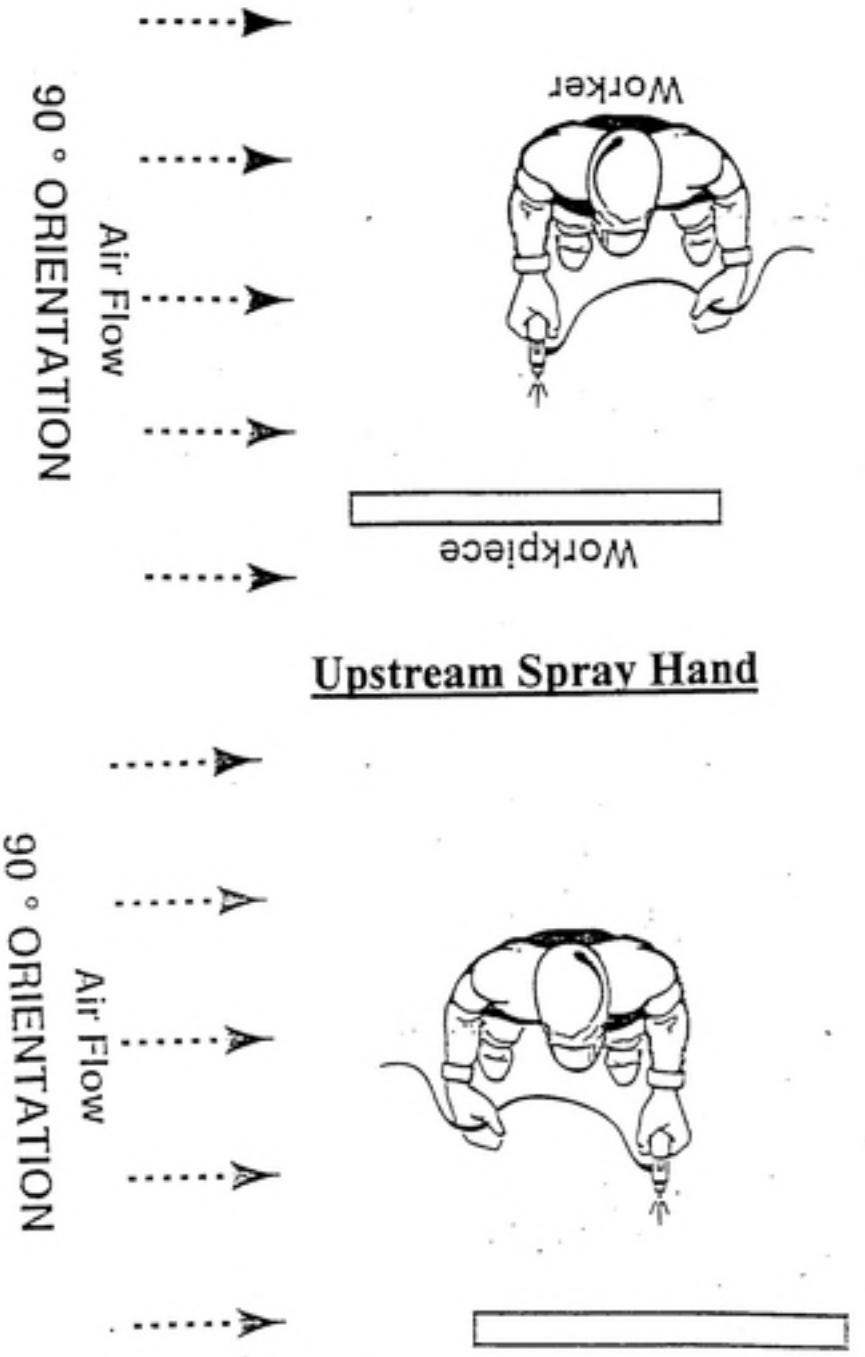

Figure 3: Spray Gun Hand Orientation

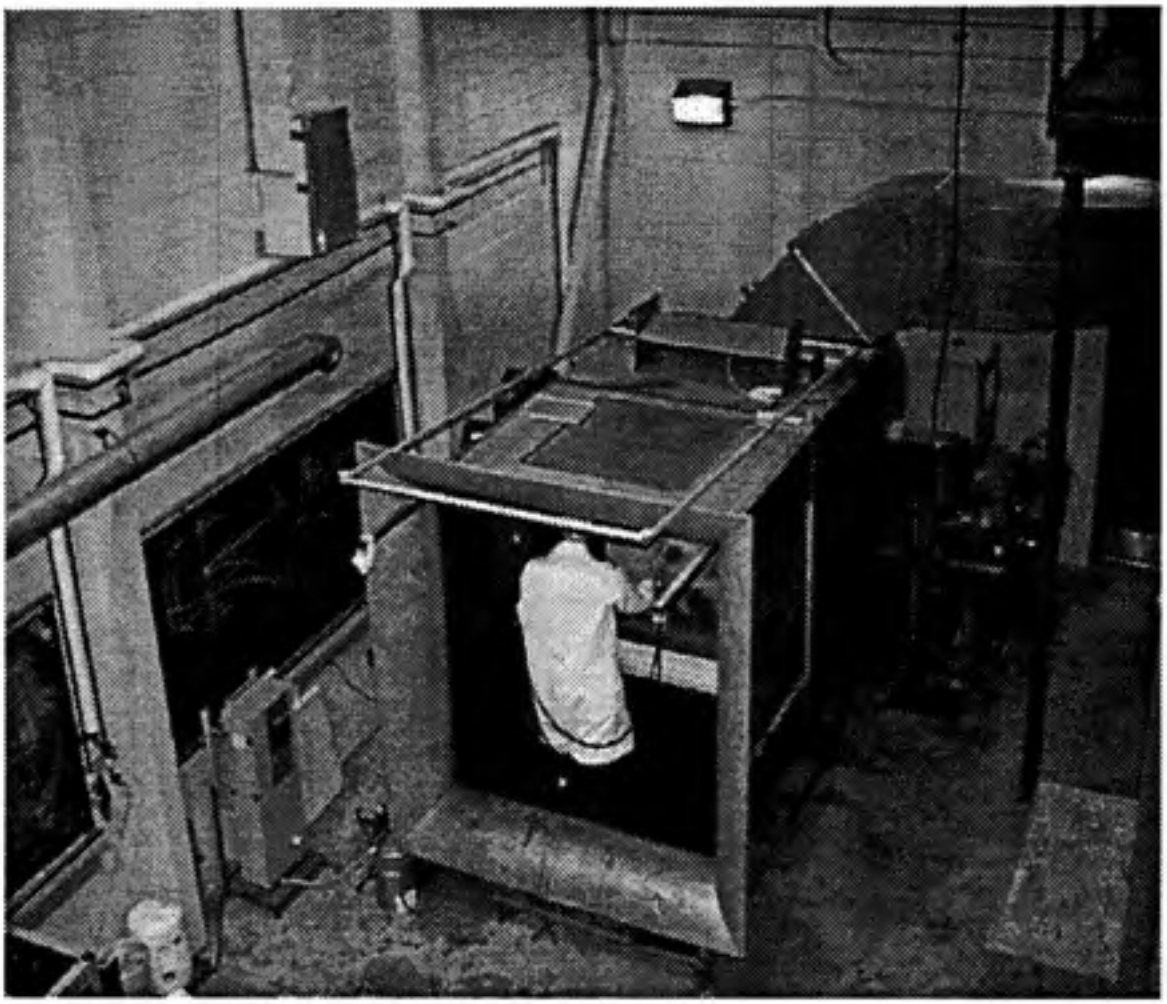

Figure 4: Experimental Setup

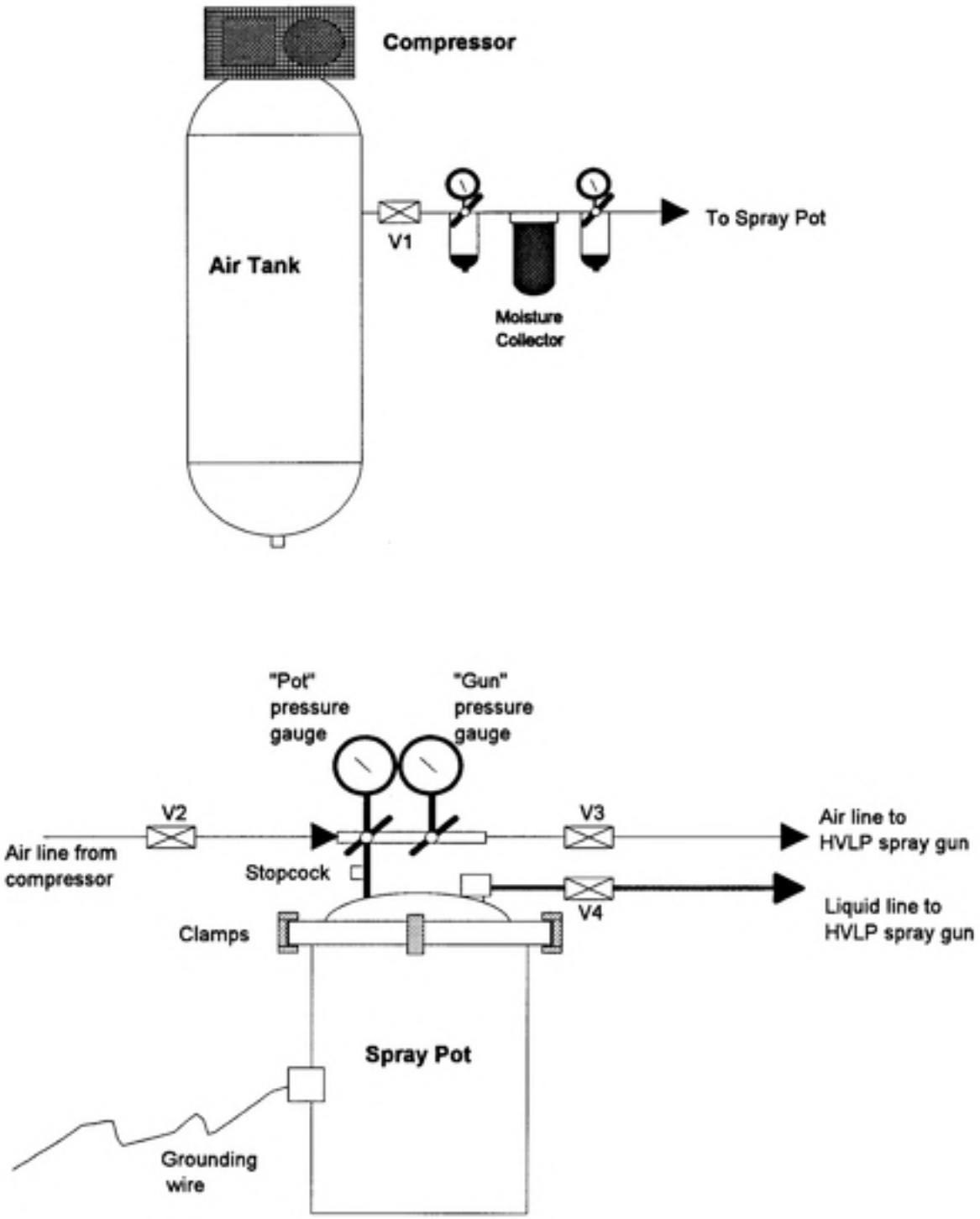

Figure 5: Schematic of Compressor and Spray Pot Systems

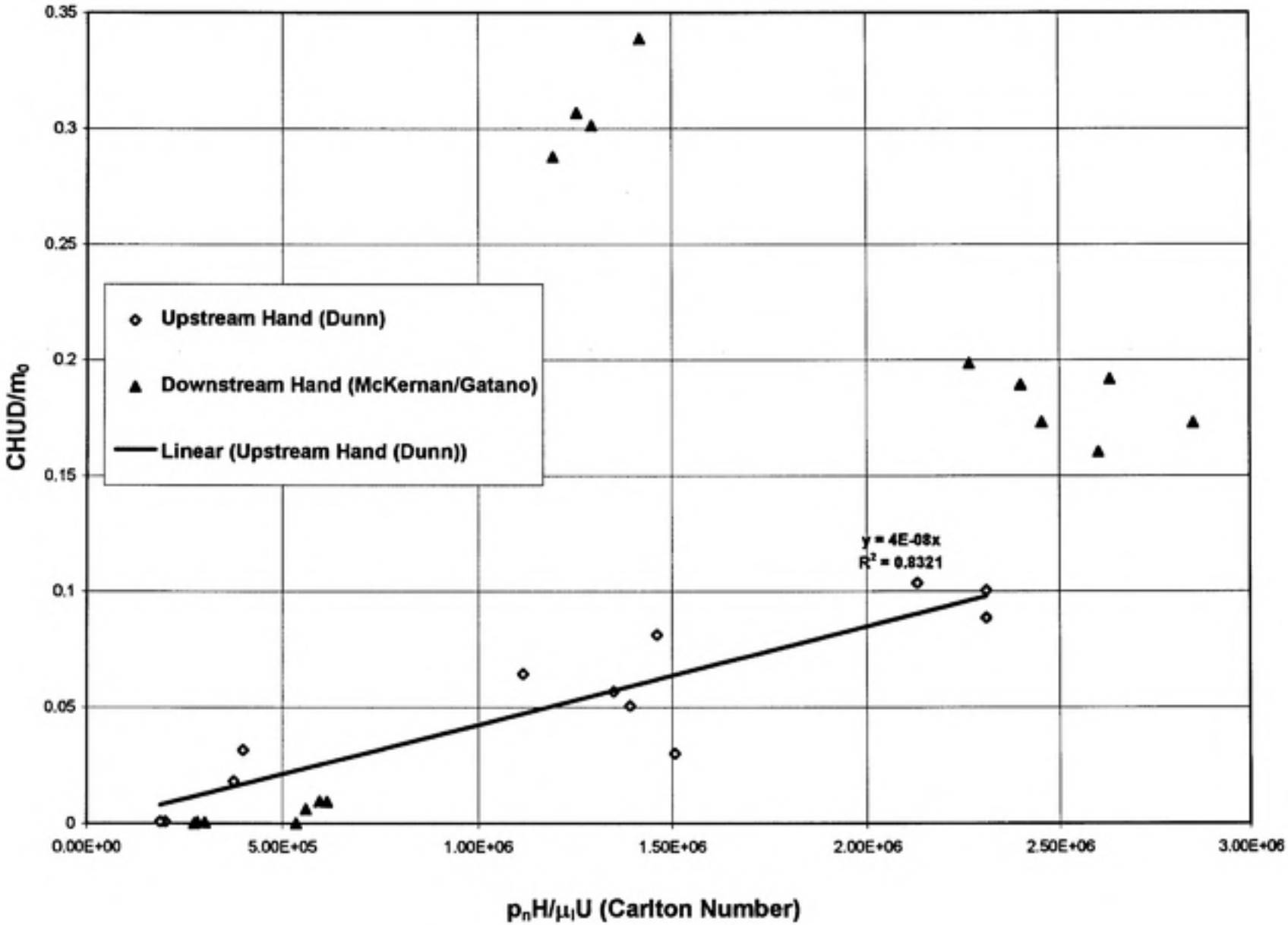

Figure 6: The Effects of Upstream versus Downstream Handedness

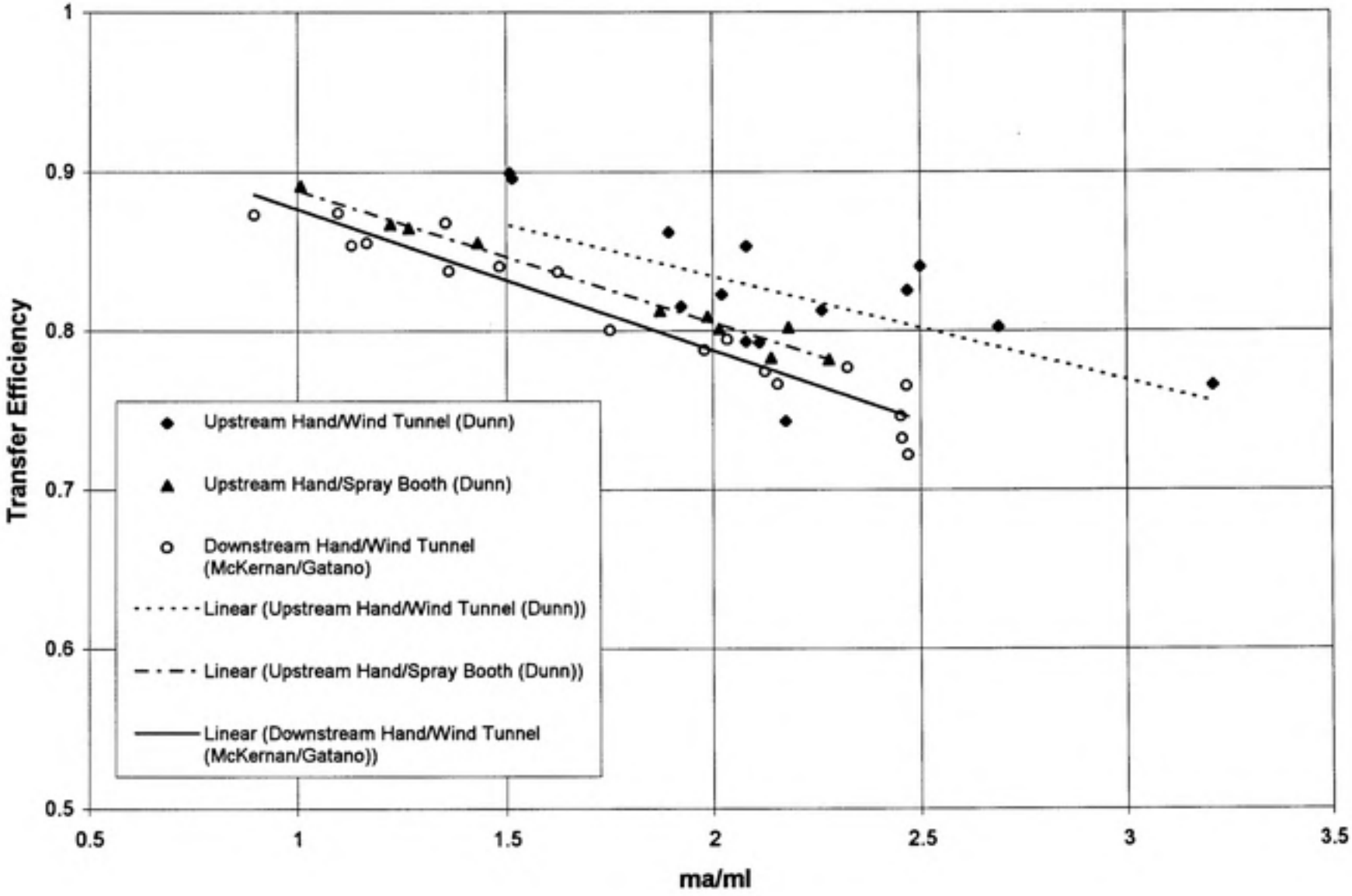

Figure 7: Transfer Efficiency as a Function of the Ratio of Mass Flowrates of Air to Liquid (m_a/m_l)

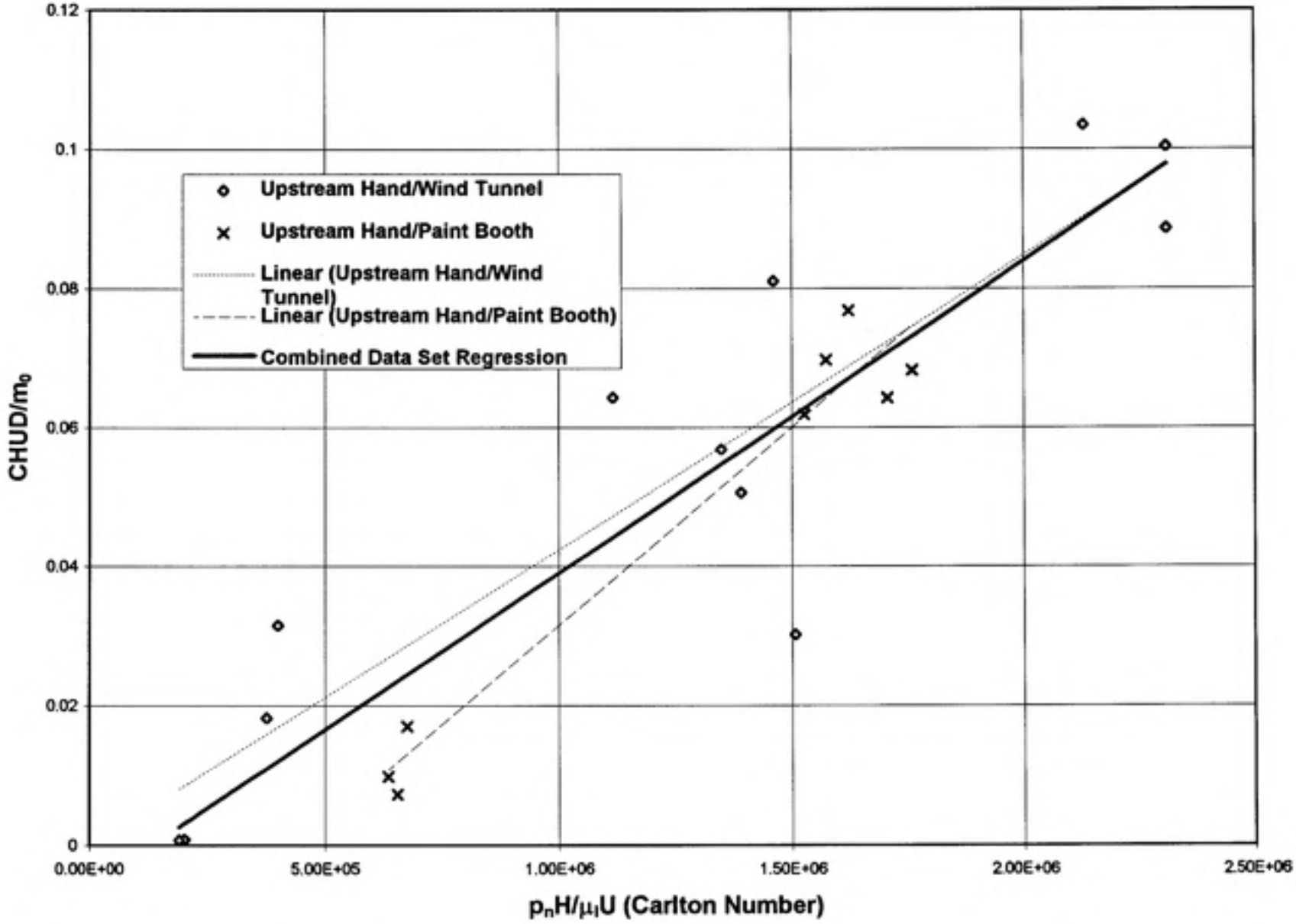

Figure 8 - Effects of wind tunnel blockage on test results

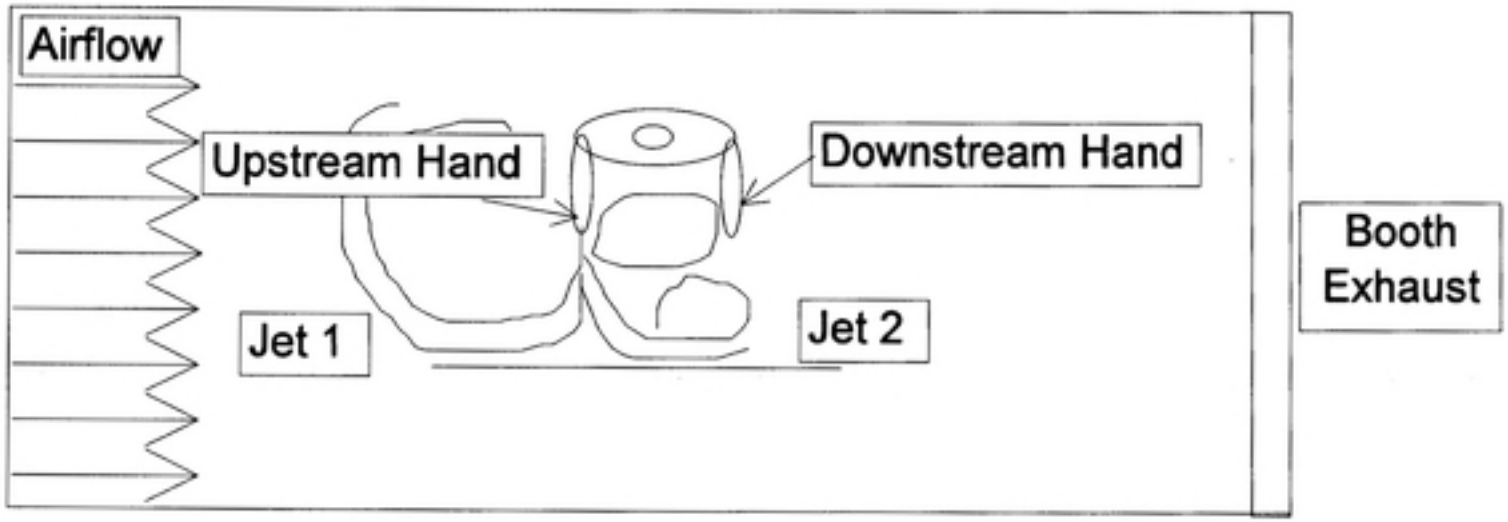

Figure 9: Diagram of Overspray Pattern

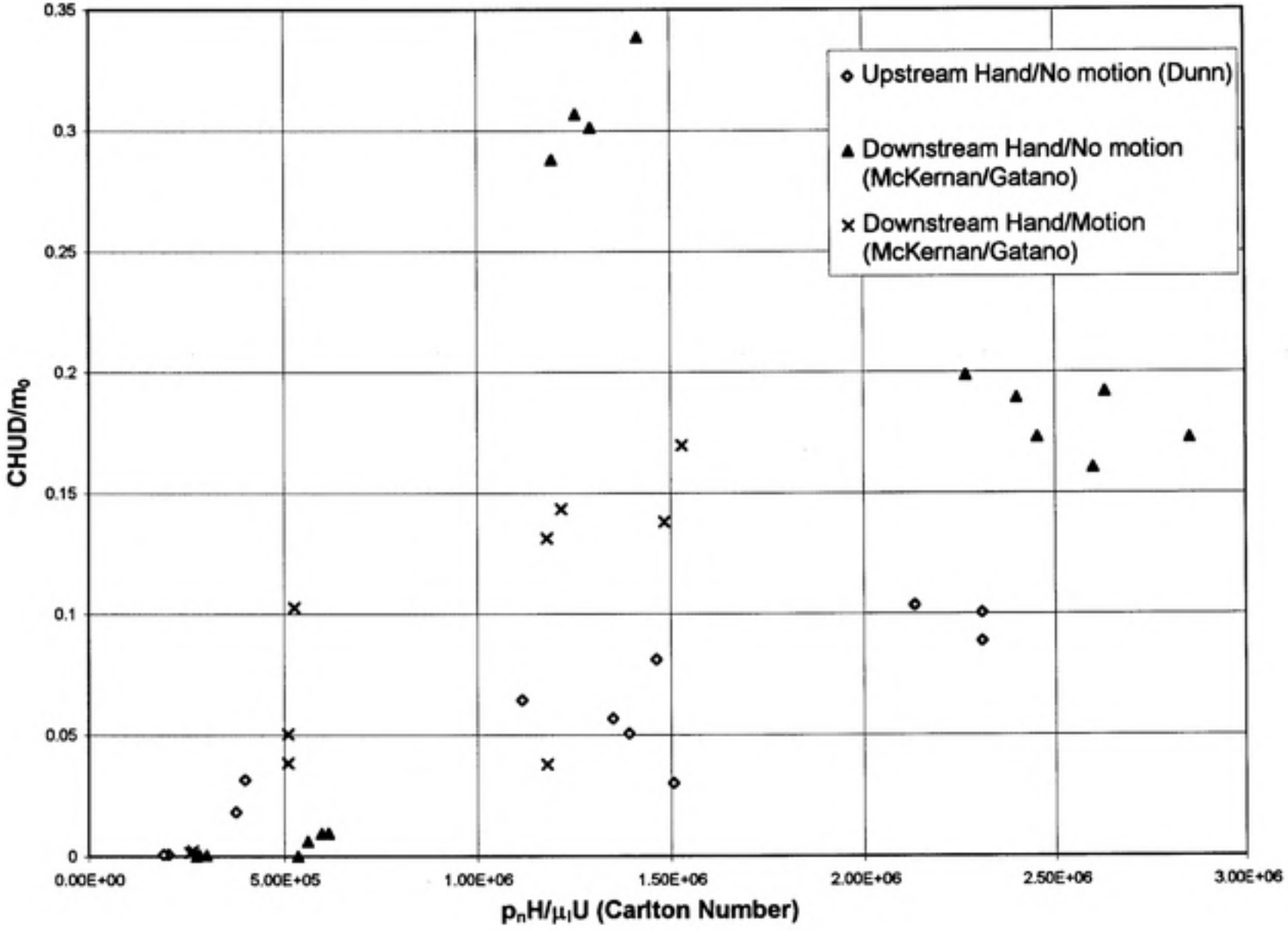

Figure 10: Comparsion of the Effects of Motion on Downstream Hand Concentrations

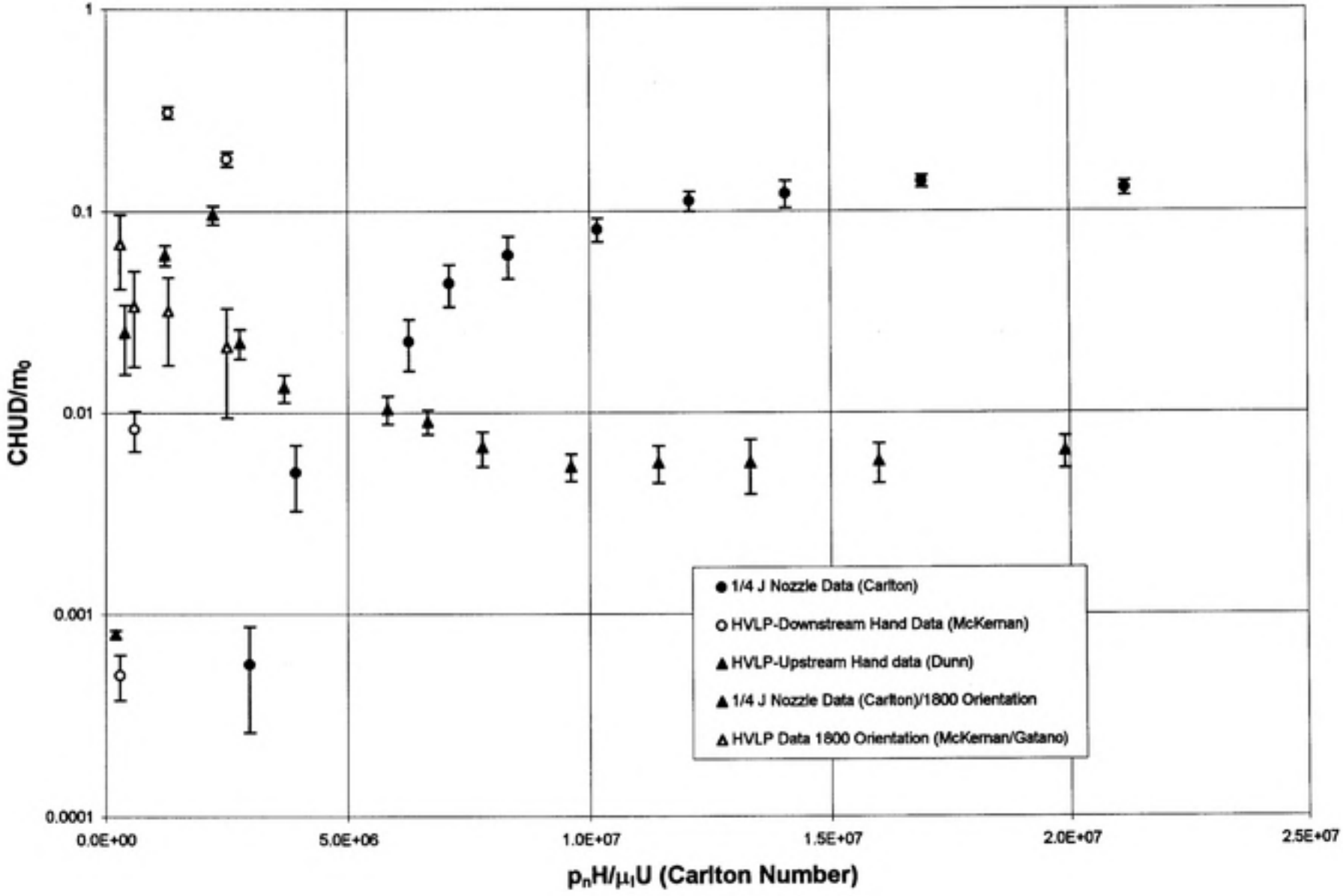

Figure 11: Functional relationship between the dimensionless groups for all Data Sets

Table 1: Wilcoxon Statistical Test Results for the Effects of Lapel Sample Location

Run #	Carlton #	Concentration		Difference	Rank	"+" Ranks	"-" Ranks	%Diff
		Upstream	Downstream					
1	2.31E+06	232.88	273.68	40.80	10	10	0	14.9
4	2.13E+06	169.01	258.56	89.56	11	11	0	34.6
5	1.51E+06	68.92	73.02	4.10	3	3	0	5.6
6	1.39E+06	63.90	80.47	16.58	7	7	0	20.6
7	1.46E+06	94.54	117.27	22.73	9	9	0	19.4
8	1.35E+06	61.28	69.57	8.30	6	6	0	11.9
9	2.03E+05	0.17	0.35	0.17	2	2	0	49.7
10	4.00E+05	14.28	21.23	6.95	5	5	0	32.8
12	1.91E+05	0.24	0.32	0.07	1	1	0	22.7
13	3.77E+05	5.05	11.88	6.84	4	4	0	57.5
14	1.11E+06	69.56	86.88	17.32	8	8	0	19.9
						66	0	

Table 2: Blockage Ratio Comparison between Paint Booth and Wind Tunnel

	Experimental Wind Tunnel	Paint Booth
Cross sectional area of test section (ft^2)	25	45
Projected area of test article (ft^2)	5.44	5.44
Blockage ratio	0.22	0.12

Appendix A: Wind Tunnel Experimental Methods and Data

A.1. ThermoAnemometer Calibration

An Alnor Compuflow® model 8565 ThermoAnemometer was used throughout this project to measure air velocity. The unit is a portable hand-held instrument capable of measuring velocities from 20-3000 fpm. The thermal anemometer uses both a velocity sensor and temperature sensor. The velocity sensor is a fine nickel wire located in the probe tip heated with a constant current. As air passes over the velocity sensor, the sensor is cooled and a change in resistance occurs. The air speed has been shown to be proportional to the change in resistance of the velocity sensor. The anemometer was calibrated in a small wind tunnel with a cross sectional area of 2.56 ft^2. The calibration setup is shown in Figure A.1. A bell shaped streamline entry was used to provide uniform flow into the test section. A screen was also placed in the back of the test section to assist in maintaining uniform flow across the calibration wind tunnel. An electronically controlled butterfly damper valve provided flow regulation across the range of required airstream velocities.

Volumetric airflow was measured by a calibrated orifice connected to an inclined manometer. Atmospheric conditions were also recorded including wet and dry bulb

temperature (sling psychrometer) and barometric pressure (Fischer-Scientific barometer). The calibration was performed in accordance with ACGIH recommended practice for the calibration of air measuring instruments.[3] The results of this calibration are shown in Table A.1. A least squares linear regression was performed to fit the data. The calibration curve is shown in Figure A.2. The applicable regression equation is:

$$\text{Actual velocity (fpm)} = 1.0848\ (\text{Reading}_{\text{instrument}}) - 9.5625,\ r^2 = 0.999 \qquad (1)$$

A.2. Orifice Flowmeter Calibration

A sharp-edged orifice was used to measure volumetric airflow through the calibration wind tunnel. The orifice meter was calibrated using the test setup as described in the previous paragraph (see Figure A.1.). The orifice was mounted between flanged ducting sections and gaskets were used to seal the installation. A pressure tap on either side of the orifice was connected to a Dwyer No. 400 Air Velocity Meter (inclined manometer) for measurement of differential pressure during calibration. The Dwyer manometer has a range of 0-10 in w.g. with a resolution of 0.01 in w.g. from 0-1 in. w.g. The orifice flowmeter causes an increase in airspeed by using a sharp edged flow obstruction, typically a flat plate with a beveled edge on the downstream side. The airflow can then be determined by the measurement of the resultant change in static pressure across the orifice and using the conservation of momentum equation to relate this differential pressure with the volumetric flowrate. A six point pitot tube traverse was

performed in accordance with ACGIH guidelines to provide actual airflow measurement.[3] Two traverses across the duct diameter made at right angles were performed to carefully map out the velocity distribution and agreements between the traverses were easily within the standard of 10%. The traverses were taken at a distance greater than the recommended standard of 7.5 duct diameters downstream of any major flow disturbance. These measurements were taken at eight distinct orifice differential pressures corresponding to airflows within the range of interest (100-900 cfm). The results of this calibration are shown in Table A.1.

A.3. Calibration of the Experimental Wind Tunnel

Airstream velocity through the experimental (large) wind tunnel is one of the primary variables of interest in this project. A sixteen point traverse was performed across the tunnel cross section. A bank of filters were installed on a pegboard in the rear of the tunnel to assist in maintaining uniform airstream velocity throughout the tunnel. A bell shaped entry was also installed on the tunnel to minimize the effects of flow separation cause by a vena contracta on the tunnel entrance. The flowrate through the tunnel is adjustable by varying the speed of the fan via a Toshiba Tosvert model 130H1 variable torque transistor inverter. See Figure A.4. for the experimental wind tunnel setup.

The air velocity was measured by the thermo-anemometer on a 16 point grid across a range of tunnel static pressures. The tunnel static pressure was measured by a

pitot tube installed in the exhaust duct downstream of the tunnel exit prior to the fan. A Dwyer Model No. 424 Air Velocity Meter (inclined manometer) was used to measure the tunnel static pressure throughout the experiment. The freestream velocity (U) was determined from the average of the sixteen readings and was regressed on the square root of the tunnel static pressure as shown in Figure A.4. A linear regression of the dataset yielded a best fit equation:

$$\text{Freestream Velocity (U)} = 403.75\ (SP_{tunnel})^{1/2},\quad r^2 = 0.9995 \qquad (2)$$

A.4. Vacuum Pump Oil Viscosity

The vacuum pump oil viscosity was measured using a Haake falling ball viscometer with a constant temperature bath. Viscosity measurements were taken at nine temperatures ranging from 20° C to 36°C. Agraph of the results of these measurements is shown in Figure A.5. A best fit regression equation for viscosity is:

$$\text{Viscosity (cp)} = 678.95\ \exp[(-0.0306)\text{Temperature}(^0\text{F})],\quad r^2 = 0.9988 \qquad (3)$$

A.5. Experimental Setup

The HVLP spray painting setup is shown in Figure A.6. A photograph of the compressor and spray paint system is shown in Figure A.7. The pressure at the

compressor /accumulator exit was set to 100 psi and the regulator downstream of the desiccator was set to 90 psi. The compressor was set to start if the pressure in the accumulator dropped to 140 psi or lower so that a constant delivery pressure was maintained. The "gun" pressure regulator was fixed and not altered throughout the testing, rather the "pot" pressure regulator was adjusted to vary the nozzle pressure and thus the air flowrate from the gun. A calibration of the "pot" pressure versus gun air cap pressure was performed using an air cap test kit. This test kit allows the user to check the air pressure at the center and fan air ports to verify that the required pressure exists to provide adequate atomization. The results of this test are shown in Table A.2.

The HVLP gun has two adjustment screws on the spray gun body to allow the user to adjust the air or liquid flowrates (see Figure A.8). Typically, the air adjustment screw is used to vary the fan pattern of the gun. The operator adjusts the fan pattern based on the shape of the part being coated to minimize overspray and reduce material usage. The liquid adjustment screw is sometimes also changed to impart the desired coating thickness to the part. In this project, the fan pattern was set to emulate that of a ellipse, which is used frequently throughout industry. A calibration was also performed to measure the spray gun airflow at each "pot" regulator setting. The airflow was measured using a Collins P-1700-120 chain-compensated 120 liter spirometer. The time required to displace a known volume of air from the gasometer was measured. Measurements were made across a range of "pot" gauge pressures and subsequent air cap pressures between 2.5 - 11.5 psi. The measurements were also repeated for a series of three air adjustment

screw settings (1-3 complete rotations). The results of these tests are listed in Table A.3. and shown graphically in Figure A.9. The linear regression equation relating spray gun airflow to air cap pressure is :

Volumetric Flowrate (cfm) = 1.0076(air cap pressure, psi) + 5.1589, $r^2 = 0.9863$ (4)

A.6. Calibration of the Sample Pump

The mannequin breathing zone concentration was determined by sampling for the aerosol via NIOSH Method 0500. An IOM sampler was utilized to minimize the effects of particle size on inlet efficiency. The sampling pump used was an SKC Universal Flow Sample Pump Catalog No. 224-PCXR8. This pump is equipped with a rotameter mounted on the case to allow the user to monitor the flow throughout sampling. The electrical control system also has a constant flow system which increases motor voltage as the back pressure increases. This provides for constant flow even as the back pressure of the filter increases due to loading.

The pump and sampler was calibrated before and after each run. This assured that significant drift could not affect the volume of air sampled and therefore the measured concentration. An open faced sampler calibration setup was used to perform the pump/sampler calibrations. The combined pump and sampler (with filter & backing pad) was calibrated together to account for the effect of sampler pressure drop on the sample

flowrate. A Gilian Gillibrator (bubble flowmeter) with a 0-2 lpm cell was the primary standard used to perform the pump calibration.

A.7. Filter and Vacuum Oil Weights

The PVC 37 mm sampling filters were placed in a desiccator for a period of at least 2 hours prior to and following sampling. The filters were weighed on a Cahn 27 Electrobalance on the 20 Loop A setting which has a range of 0-20 mg with a resolution of 1μg. The sensitivity of the balance is reported to be 0.0001 mg with an accuracy of ±0.005%. The balance was zeroed and calibrated with a 200 mg Class M calibrating weight in accordance with manufacturer's specifications before each series of experimental runs. A radioactive ionizing unit was passed over the filters before weighing to discharge any static electricity buildup on the filter which may cause erroneous readings.

The mass of liquid used during the experimental runs and the mass transferred to the plate was measured by a mass balance method. The liquid feed pot was weighed prior to each run and following the completion of each run. The amount of liquid transferred was measured by the weighing of the drip trough placed underneath the plate before and after each run. A Mettler PM34-K Deltarange digital scale was used to measure the quanities of liquid used and transferred. The Mettler scale was calibrated at the factory and was in calibration during the entire period of testing. The scale was zeroed, as necessary, before each measurement.

A.8. Experimental Data

The experimental identification table is shown in Table A.4. This table shows the conditions under which the test run was performed including data such as environmental conditions, freestream velocity (U), mannequin orientation, nozzle pressure (p_n) breathing zone concentration (BZC) sample location, and dimensionless nozzle pressure (Carlton number). Two concentration samples were collected for each run and are given the designation A or B. The calculated overspray data is shown in Table A.5. This table includes information such as mass flow rates of air and liquid, mass of liquid transferred, and overspray generation rate (m_0), and transfer efficiency. The breathing zone concentration data is shown in Table A.6. This table includes information such as sample filter weights, blank filter weights, and calculated dimensionless concentration. Samples # 2A and 3A were taken from the mannequin mouth and problems with the test setup prevented the collection of adequate sample mass for analysis. These samples were therefore excluded from analysis. Run #11 was not included in the analysis as the sample mass was much greater than the limits specified in NIOSH Method 0500. Sample calculations are shown in section A.11 below.

A.9. Sample Calculations (for Run Number 1)

A.9.1 m_a/m_l

The measured value of m_a , at total nozzle pressure = 11.5 psi was 285 g/min.

$$m_l = \frac{\text{mass container(before)} - \text{mass container(after)}}{\text{sampling time}}$$

$$= \frac{(3400.9 - 2986.8)g}{183.97\ \text{sec}} \times \left(\frac{60\ \text{sec}}{\text{min}}\right) = 135.1\ \text{g/min}$$

$$\frac{m_a}{m_l} = \frac{285\ \text{g/min}}{135.1\ \text{g/min}} = 2.1$$

A.9.2 Transfer Efficiency

$$m_{transferred} = \frac{\text{mass trough(before)} - \text{mass trough(after)}}{\text{sampling time}}$$

$$\frac{(551.9 - 223.8)g}{183.97\ \text{sec}} \times \left(\frac{60\ \text{sec}}{\text{min}}\right) = 107.0\ \text{g/min}$$

$$\text{T.E.} = \frac{\text{liquid transfer rate } (m_{transferred})}{\text{total liquid mass flowrate } (m_l)} = \frac{107.0\ \text{g/min}}{135.1\ \text{g/min}}$$

$$= 0.792$$

A.9.3 $p_n H/\mu_l U$

From equation (A-2),

Freestream Velocity (U) = $403.75\ (0.05)^{1/2}$ = 73.0 ft/min

From equation (A-3)

μ_l (cp) = 678.95 exp[(-0.0306)(75^{0}F)] = 68.41 cp

$$\frac{p_n H}{m_l U} = \frac{(6.5\text{psi})(51\text{ in})}{(68.41\text{ cp})(73.0\text{ fpm})} \times \left(\frac{\text{atm}}{14.7\text{psi}}\right) \times \left(\frac{1.01325\times10^6\text{ dynes / cm}^2}{\text{atm}}\right) \times \left(\frac{\text{ft}}{12\text{ in}}\right) \times \left(\frac{\text{cp}}{0.01\text{dyne}-\text{s/cm}^2}\right) \times \left(\frac{60\text{ sec}}{\text{min}}\right)$$

$= 2.29 \times 10^6$

A.9.4 CHUD/m_0

From sample # 1A

$$\frac{\text{CHUD}}{m_0} = \frac{(280.30\text{ mg/m}^3)(51\text{ in})(73.0\text{ ft/min})(14\text{ in})}{28.05\text{ g/min}} \times \left(\frac{1\text{ ft}^2}{144\text{ in}^2}\right) \times \left(\frac{0.02832\text{ ft}^3}{1\text{ m}^3}\right) \times \left(\frac{1\text{ g}}{1000\text{ mg}}\right)$$

= 0.1028

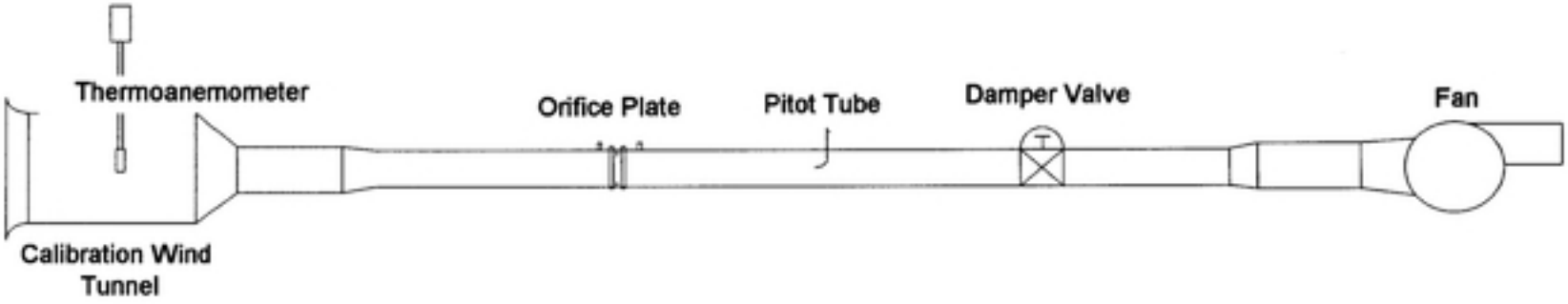

Figure A.1: Thermoanemometer Calibration Set up

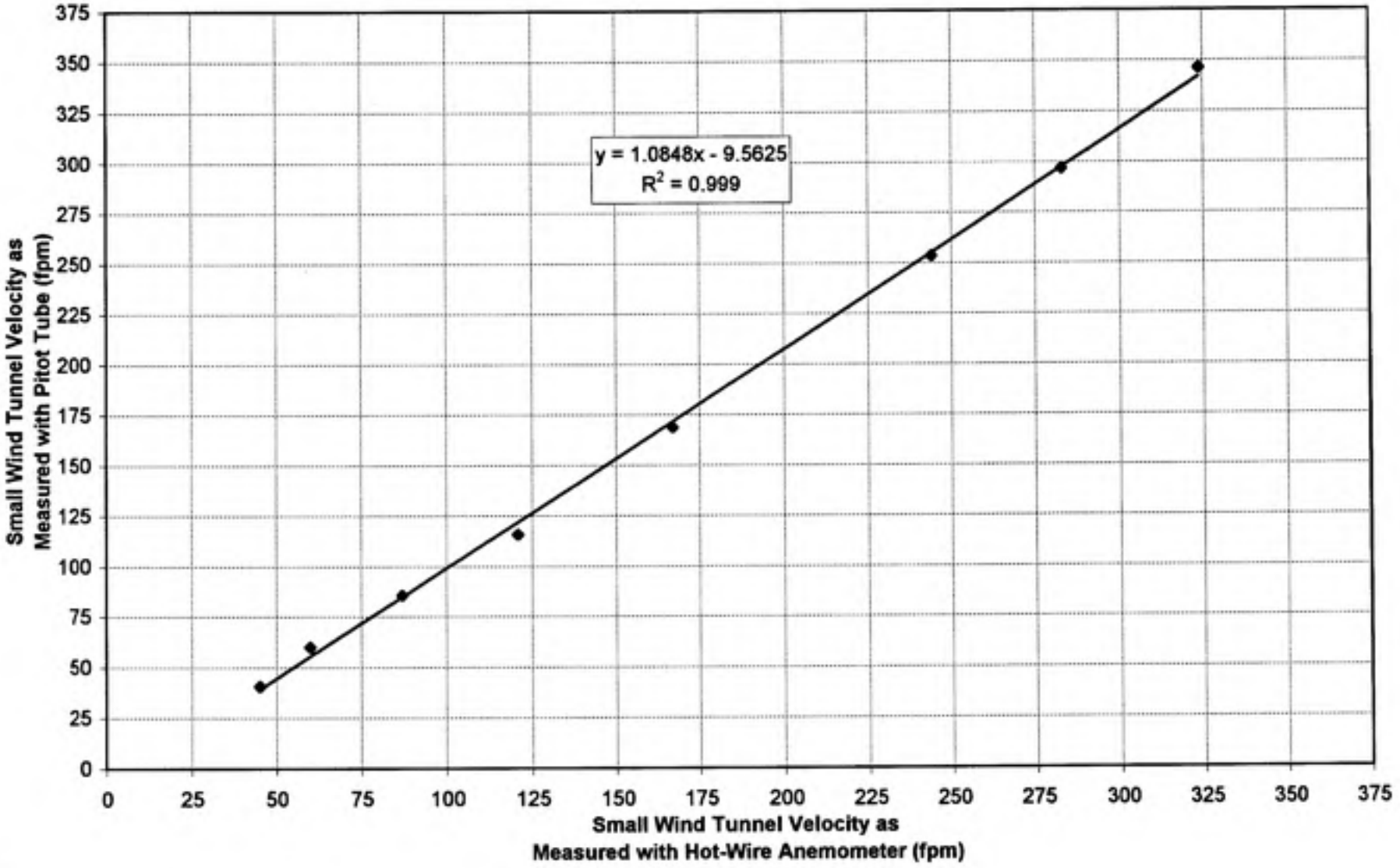

Figure A.2.: Calibration Curve for Thermo-anemometer

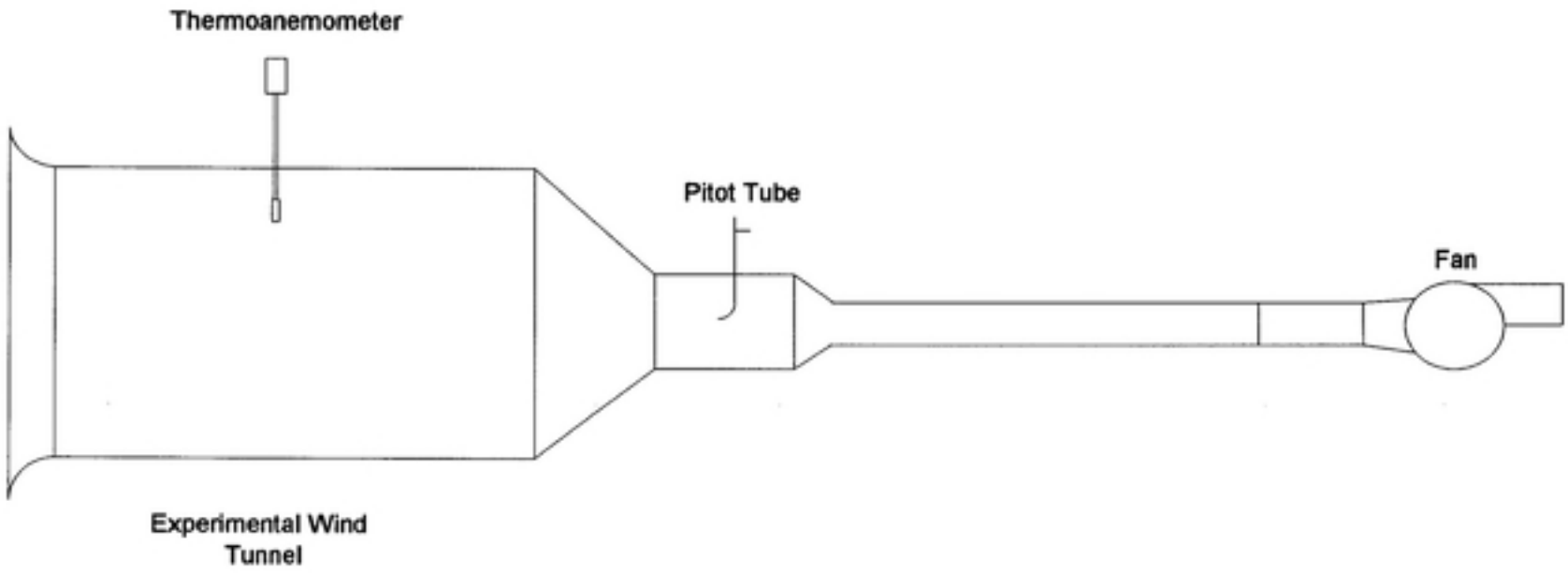

Figure A.3: Experimental wind tunnel calibration set up

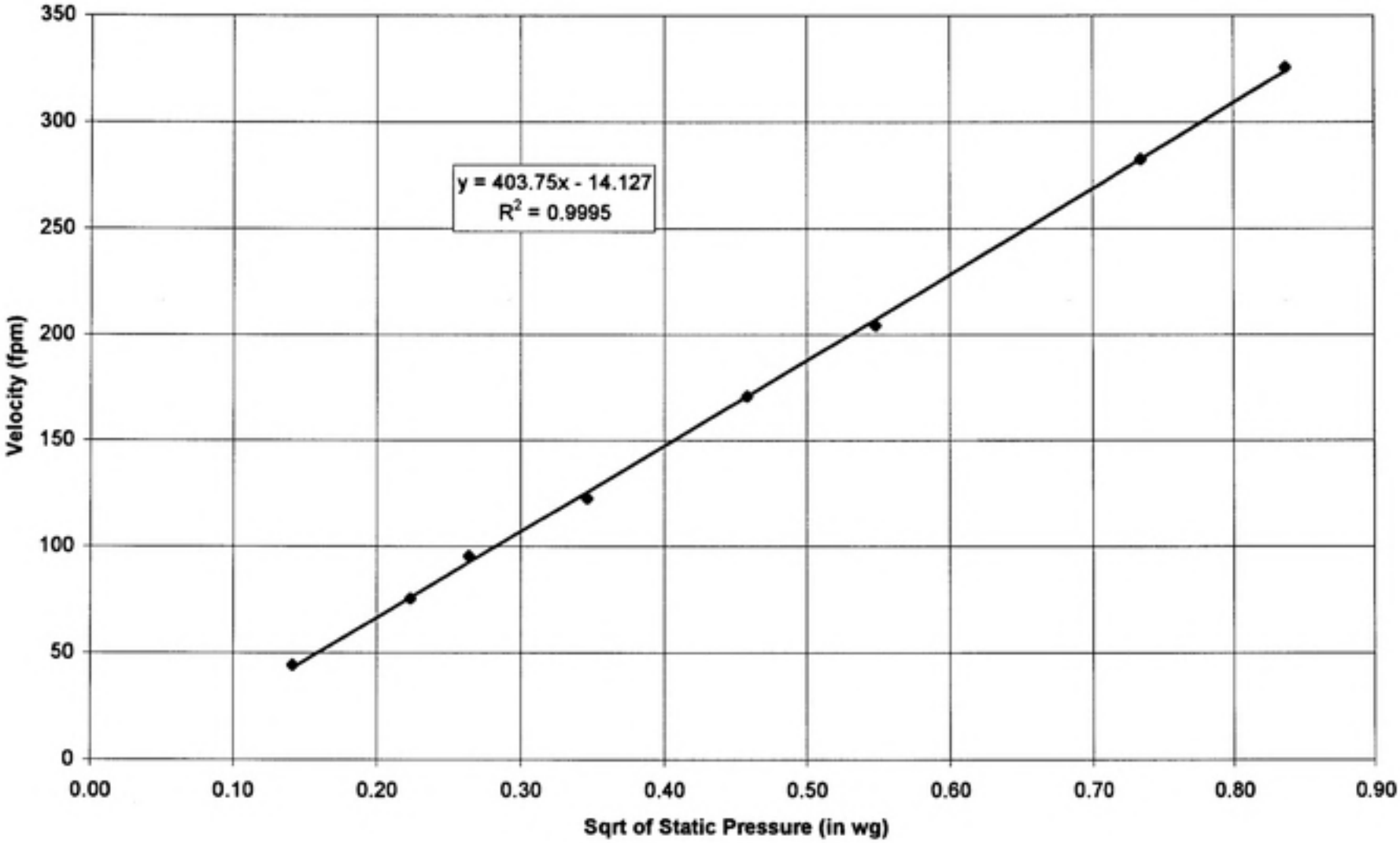

Figure A.4: Experimental Wind Tunnel Air flow Calibration Curve

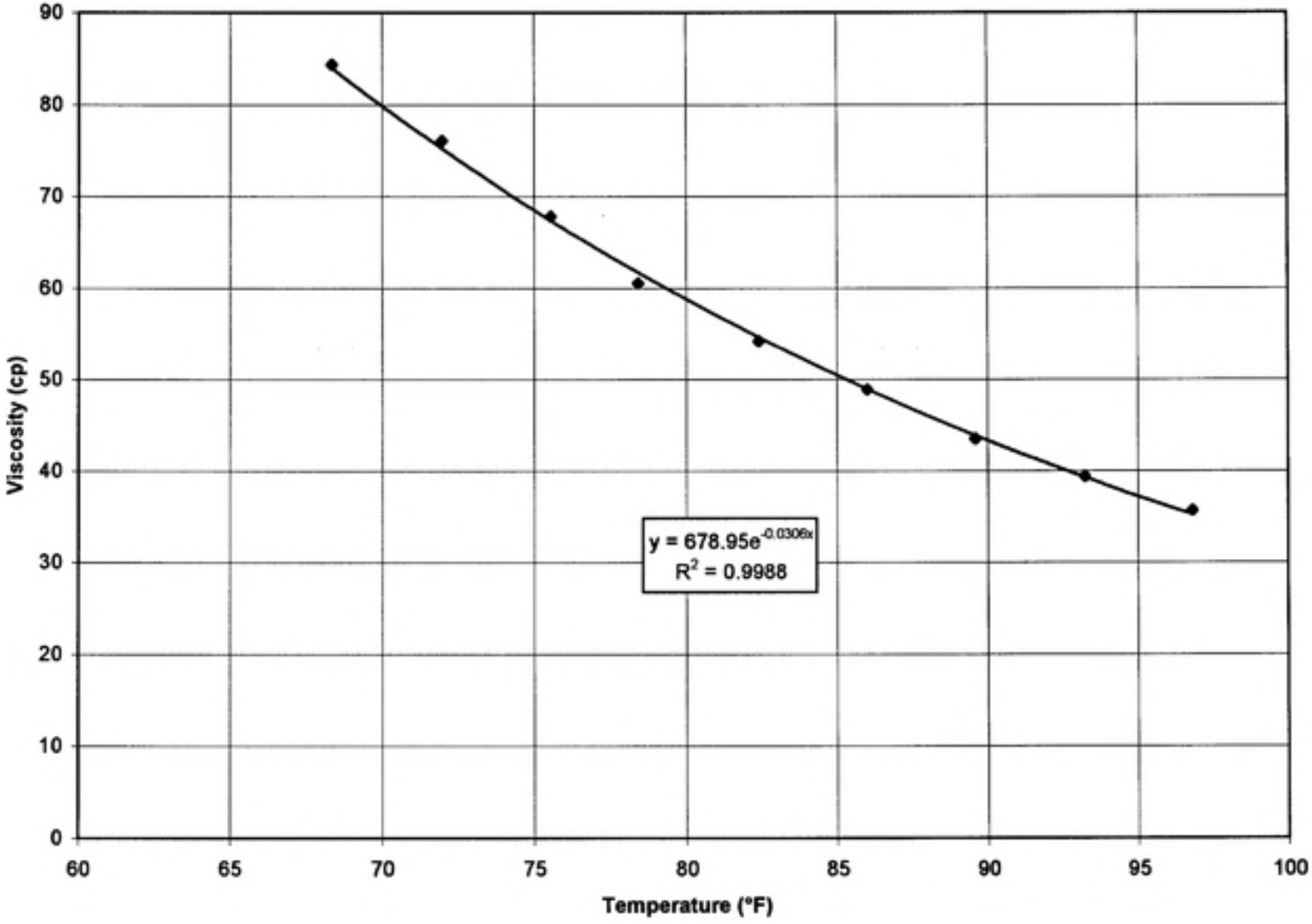

Figure A.5: Viscosity of Oil as a function of temperature

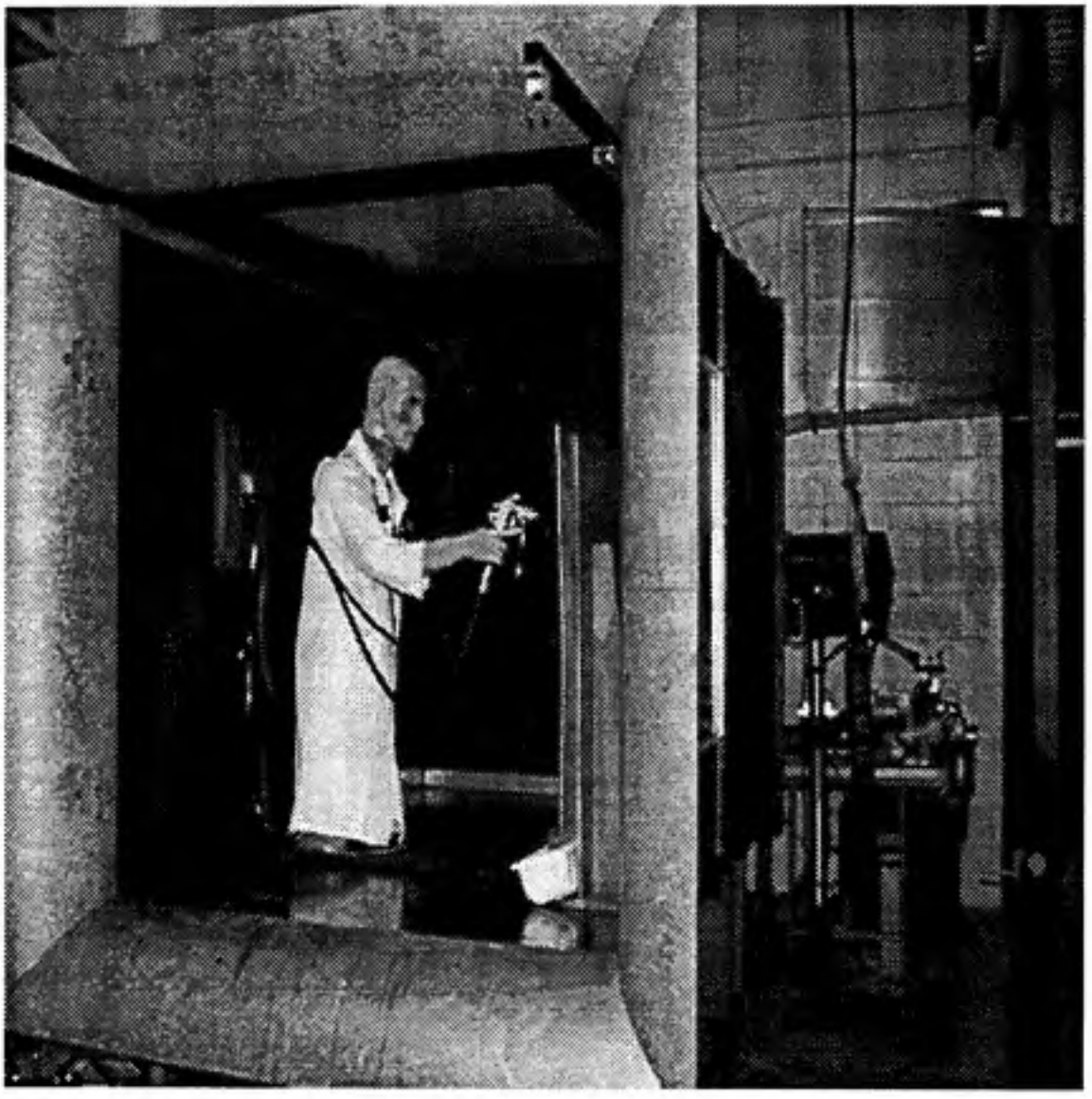

Figure A.6: Test Setup

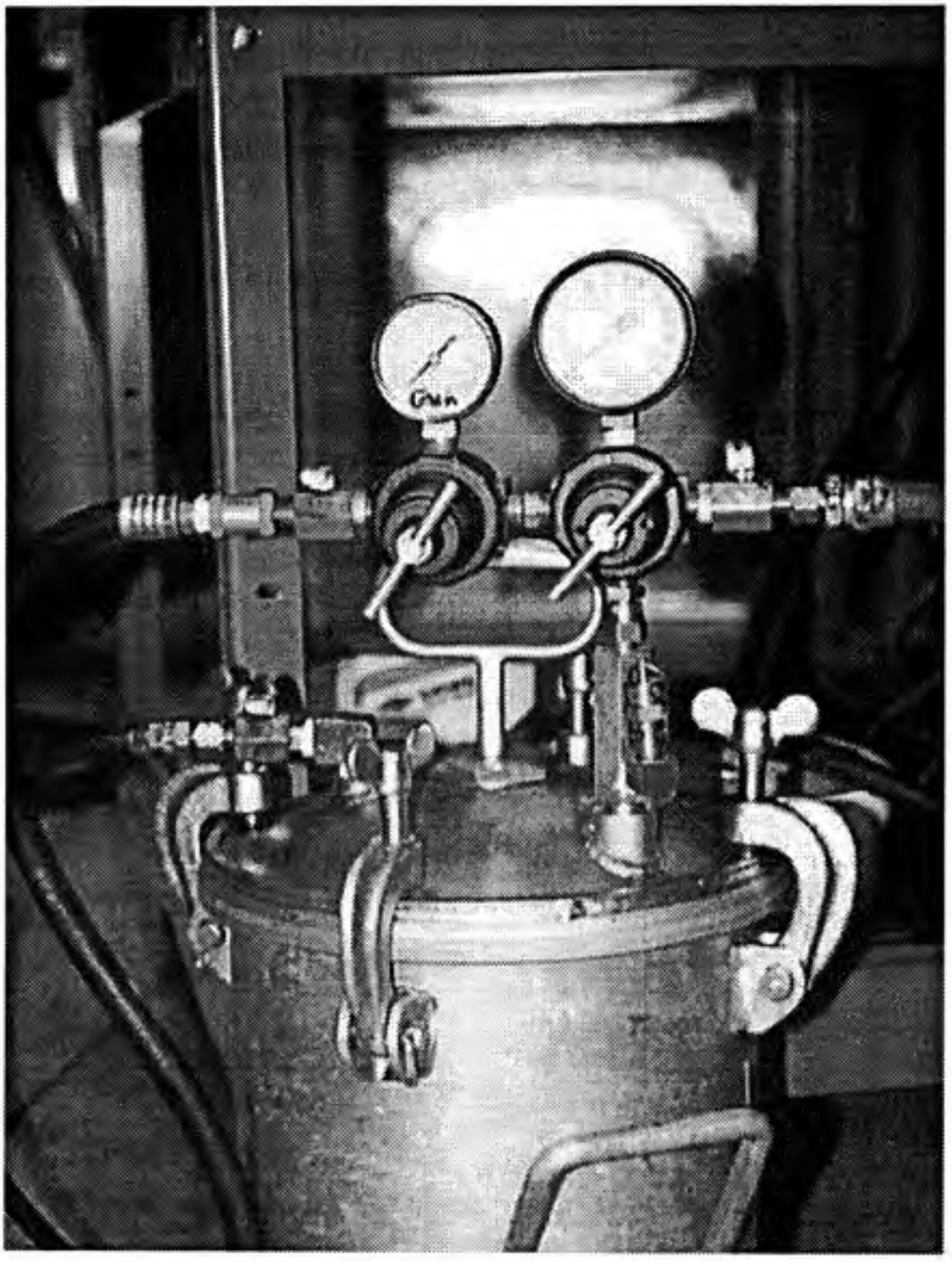

Figure A.7: Spray Pot Set Up

Figure A.8: High Volume, Low Pressure Spray Gun

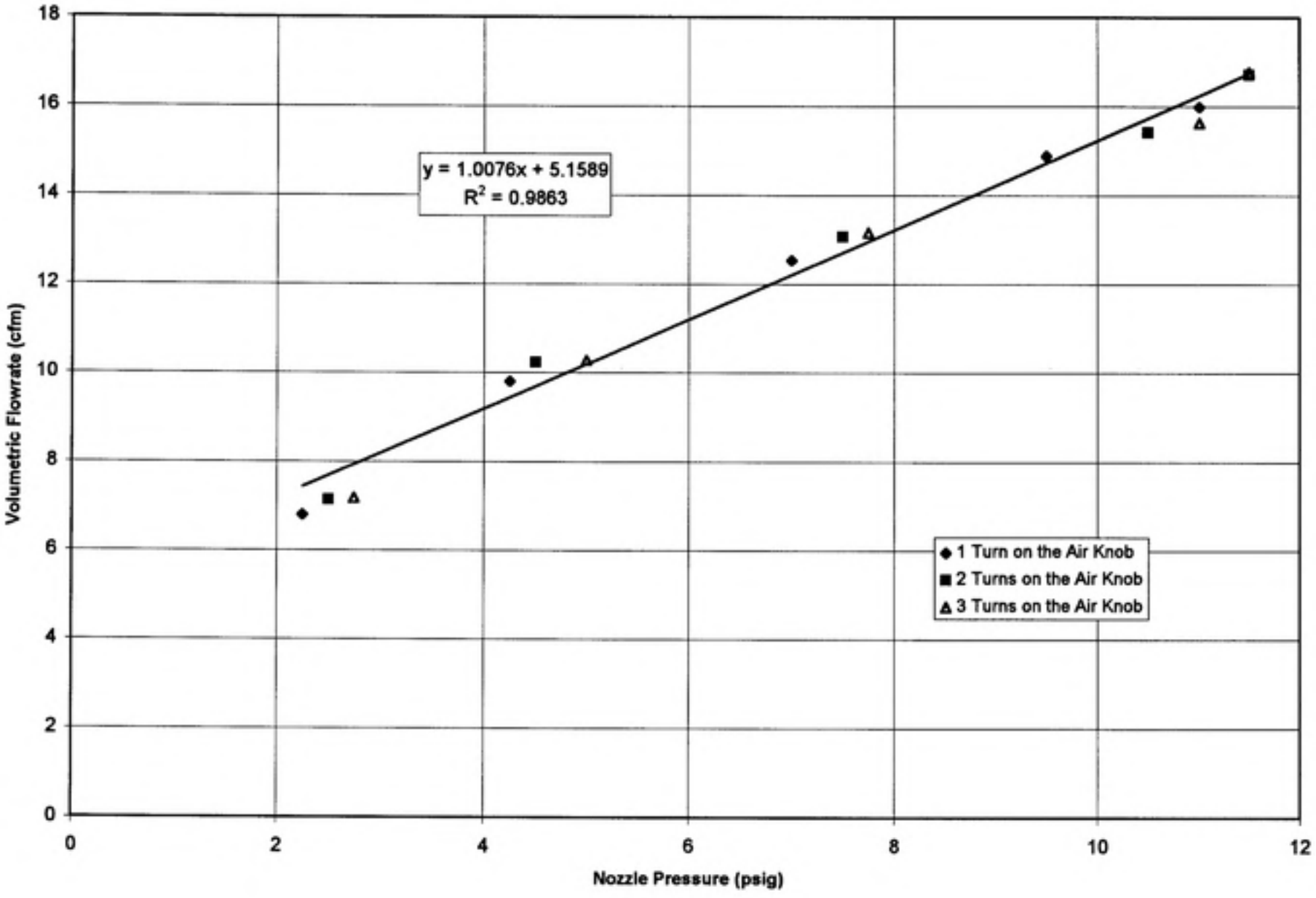

Figure A.9: Volumetric Air Flowrate from the HVLP Gun as a Function of Nozzle Pressure and Fan Pattern

Table A.1.: Thermo-anemometer and Orfice Calibration Data

Orifice Pressure (in wg)	SQRT (Orifice Pressure (in wg)	Velocity in Duct (fpm)	Air Volume (Q), CFM	Velocity in Small Wind Tunnel (fpm)	Direct Reading Thermal Anemometer (fpm)
0.10	0.32	1184	103	41	45
0.20	0.45	1750	153	60	60
0.50	0.71	2495	218	86	87
1.00	1.00	3367	294	116	121
2.00	1.41	4909	428	169	167
5.00	2.24	7379	644	254	244
7.00	2.65	8637	754	297	283
9.80	3.13	10076	879	346	324

Table A.2 Determination of Air Pressure at the Cap and the Horns

Gauge Pressure (psig)	Number of Turns on Air Knob	Pressure in Cap (psig)	Pressure in Horns (psig)
53	0	10	0
53	1	7	4
53	2	6.5	5
53	3	6.5	5
46	0	8	0
46	1	6	3.5
46	2	6	4.5
46	3	6	5
38	0	6	0
38	1	4.25	2.25
38	2	4.25	3.25
38	3	4.5	3.5
27	0	4	0
27	1	2.75	1.5
27	2	2.5	2.0
27	3	3.0	2.0
16	0	2	0
16	1	1.75	0.75
16	2	1.5	1.0
16	3	1.75	1.0

Table A.3 - Spray Gun Volumetric Airflow versus Air Cap Pressure

	Average Volumetric Flowrate (cfm)		
Nozzle Pressure (psig) Tot=Cap + Horn	1 turn	2 turn	3 turn
11	15.99		
11.5		16.71	
11.5			16.76
9.5	14.89		
10.5		15.42	
11			15.63
7	12.54		
7.5		13.07	
7.75			13.17
4.25	9.8		
4.5		10.24	
5			10.28
2.25	6.79		
2.5		7.13	
2.75			7.17

Table A.4: Experimental Identifier Sheet

Run Number	Static Pressure (in wg)	Freestream Velocity (fpm)	Liquid Temperature (F)	Viscosity (cp)	Air Temperature (F)	Gauge Pressure (psig)	Nozzle Pressure Cap (psig)	Nozzle Pressure Cap&Horn (psig)	Sample Location
1A	0.05	73.0	75	68.41	81	53	6.5	11.5	Upstream
1B	0.05	73.0	75	68.41	81	53	6.5	11.5	Downstream
2A	0.05	73.0	75	68.41	81	53	6.5	11.5	Mouth
2B	0.05	73.0	75	68.41	81	53	6.5	11.5	Downstream
3A	0.05	73.0	75	68.41	81	46	6	10.5	Mouth
3B	0.05	73.0	75	68.41	81	46	6	10.5	Downstream
4A	0.05	73.0	75	68.41	81	46	6	10.5	Upstream
4B	0.05	73.0	75	68.41	81	46	6	10.5	Downstream
Blank									
5A	0.08	99.0	71	77.32	74	53	6.5	11.5	Upstream
5B	0.08	99.0	71	77.32	74	53	6.5	11.5	Downstream
6A	0.08	99.0	71	77.32	74	46	6	10.5	Upstream
6B	0.08	99.0	71	77.32	74	46	6	10.5	Downstream
Blank									
7A	0.08	99.0	70	79.72	70	53	6.5	11.5	Upstream
7B	0.08	99.0	70	79.72	70	53	6.5	11.5	Downstream
8A	0.08	99.0	70	79.72	70	46	6	10.5	Upstream
8B	0.08	99.0	70	79.72	70	46	6	10.5	Downstream
Blank									
9A	0.16	150.3	67	87.39	66	16	1.5	2.5	Upstream
9B	0.16	150.3	67	87.39	66	16	1.5	2.5	Downstream
10A	0.12	126.8	67	87.39	66	27	2.5	4.5	Upstream
10B	0.12	126.8	67	87.39	66	27	2.5	4.5	Downstream
11A	0.08	99.0	67	87.39	66	46	6	10.5	Upstream
11B	0.08	99.0	67	87.39	66	46	6	10.5	Downstream
Blank									
12A	0.16	150.3	65	92.90	64	16	1.5	2.5	Upstream
12B	0.16	150.3	65	92.90	64	16	1.5	2.5	Downstream
13A	0.12	126.8	65	92.90	64	27	2.5	4.5	Upstream
13B	0.12	126.8	65	92.90	64	27	2.5	4.5	Downstream
14A	0.085	102.8	65	92.90	64	46	6	10.5	Upstream
14B	0.085	102.8	65	92.90	64	46	6	10.5	Downstream
Blank									

Table A.5: Transfer Efficiency/Overspray Worksheet

Run Number	Run Time (s)	Bucket Weight (g)		Trough Weight (g)		Mass of Liquid Sprayed (g/min)	Mass of Liquid Transferred (g/min)	Mass of Liquid Overspray (m_s) (g/min)	Mass of Air (g/min)**	m_s/m_t	Transfer Efficiency	Carlton Number
		Before	After	Before	After							
1	183.97	3400.9	2986.8	223.8	551.9	135.1	107.0	28.0	285	2.1	0.792	2.3E+6
2	183.17	3302.8	2884.3	235.8	567.7	137.1	108.7	28.4	285	2.1	0.793	2.3E+6
3	182.21	3210.2	2807.8	241.2	572.4	132.5	109.1	23.4	268	2.0	0.823	2.1E+6
4	187.85	3470.9	3035	241.1	596.5	139.2	113.5	25.7	268	1.9	0.815	2.1E+6
5	241.71	3234.4	2705.9	239.7	632.4	131.2	97.5	33.7	285	2.2	0.743	1.5E+6
6	244.5	3090.2	2607.3	245.3	637.9	118.5	96.3	22.2	268	2.3	0.813	1.4E+6
7	240.74	3262.2	2798.8	235.8	618.3	115.5	95.3	20.2	285	2.5	0.825	1.5E+6
8	242.48	3170.3	2737.1	245.5	609.7	107.2	90.1	17.1	268	2.5	0.841	1.3E+6
9	723.75	3340.8	2300.4	228.4	1160.6	86.3	77.3	9.0	131	1.5	0.896	2.0E+5
10	433.06	3208.7	2579.7	251.8	794	87.1	75.1	12.0	165	1.9	0.862	4.0E+5
11	605.92	3116.4	2110.4	257.3	1064.2	99.6	79.9	19.7	268	2.7	0.802	1.2E+6
12	900.51	3142.6	1843.3	244	1412.7	86.6	77.9	8.7	131	1.5	0.899	1.9E+5
13	528.52	2988.4	2289.7	267.3	863.4	79.3	67.7	11.6	165	2.1	0.853	3.8E+5
14	302.24	2880.2	2459.8	272.9	594.8	83.5	63.9	19.6	268	3.2	0.766	1.1E+6

Table A.6: Dimensionless Concentration Worksheet

Run Number	Date	Mass of Liquid Overspray (m_o) (g/min)	Time (s)	Filter Weight (m)		Sample Mass (mg)	Sampling Flowrate (lpm)	Concentration (mg/m³)	Carlton Number	CUHD/m_o
				Before	After					
1A	10/30/96	28.05	183.97	13.133	14.741	1.608	1.87	280.30	2.3E+6	0.1028
1B	10/30/96	28.05	183.97	13.405	14.719	1.314	1.89	226.75	2.3E+6	0.0832
2A	10/30/96	28.37	183.17	13.800	13.869	0.069	1.87	12.08	2.3E+6	0.0044
2B	10/30/96	28.37	183.17	14.010	15.420	1.410	1.89	244.37	2.3E+6	0.0886
3A	10/30/96	23.45	182.21	13.180	13.175	-0.005	1.87	-0.88	2.1E+6	-0.0004
3B	10/30/96	23.45	182.21	13.300	15.471	2.171	1.89	378.25	2.1E+6	0.1659
4A	10/30/96	25.71	187.85	13.740	14.730	0.990	1.87	169.01	2.1E+6	0.0676
4B	10/30/96	25.71	187.85	13.110	14.640	1.530	1.89	258.56	2.1E+6	0.1034
Blank	10/30/96			13.401	13.404	0.003				
5A	11/6/96	33.71	240.74	13.784	14.313	0.529	1.91	68.92	1.5E+6	0.0285
5B	11/6/96	33.71	240.74	13.757	14.311	0.554	1.89	73.02	1.5E+6	0.0302
6A	11/6/96	22.16	242.48	13.964	14.458	0.494	1.91	63.90	1.4E+6	0.0402
6B	11/6/96	22.16	242.48	14.050	14.665	0.615	1.89	80.47	1.4E+6	0.0506
Blank	11/6/96			13.416	13.415	-0.001				
7A	11/7/96	20.16	240.74	13.897	14.620	0.723	1.91	94.54	1.5E+6	0.0654
7B	11/7/96	20.16	240.74	13.980	14.882	0.902	1.92	117.27	1.5E+6	0.0811
8A	11/7/96	17.07	242.48	13.820	14.292	0.472	1.91	61.28	1.3E+6	0.0500
8B	11/7/96	17.07	242.48	13.650	14.189	0.539	1.92	69.57	1.3E+6	0.0568
Blank	11/7/96			13.882	13.855	-0.027				
9A	11/19/96	8.97	723.75	13.559	13.563	0.004	1.90	0.17	2.0E+5	0.0004
9B	11/19/96	8.97	723.75	12.343	12.351	0.008	1.91	0.35	2.0E+5	0.0008
10A	11/19/96	12.03	433.06	12.580	12.776	0.196	1.90	14.28	4.0E+5	0.0212
10B	11/19/96	12.03	433.06	12.816	13.109	0.293	1.91	21.23	4.0E+5	0.0315
11A	11/19/96	19.72	605.92	12.872	18.454	5.582	1.90	290.61	1.2E+6	0.2055
11B	11/19/96	19.72	605.92	12.901	16.062	3.161	1.91	163.71	1.2E+6	0.1157
Blank	11/19/96			13.596	13.592	-0.004				
12A	11/20/96	8.70	900.51	12.906	12.913	0.007	1.91	0.24	1.9E+5	0.0006
12B	11/20/96	8.70	900.51	12.990	12.999	0.009	1.90	0.32	1.9E+5	0.0008
13A	11/20/96	11.65	528.52	12.795	12.880	0.085	1.91	5.05	3.8E+5	0.0077
13B	11/20/96	11.65	528.52	12.710	12.909	0.199	1.90	11.88	3.8E+5	0.0182
14A	11/20/96	19.55	302.24	14.330	15.000	0.670	1.91	69.56	1.1E+6	0.0515
14B	11/20/96	19.55	302.24	12.894	13.726	0.832	1.90	86.88	1.1E+6	0.0643
Blank	11/20/96			12.283	12.283	0.000				

Appendix B: Paint Booth Experimental Methods and Data

B.1. ThermoAnemometer Calibration

An Alnor Compuflow® model 8565 ThermoAnemometer was used to perform the paint booth traverse in this phase of testing. The unit is a portable hand-held instrument capable of measuring velocities from 20-3000 fpm. The anemometer was calibrated in a small wind tunnel with a cross sectional area of 2.56 ft^2 according to the procedure described in appendix section A.1.The results of this calibration are shown in Table B.1 and in Figure B.1. A least squares linear regression was performed to fit the data. The applicable regression equation is:

$$\text{Actual velocity (fpm)} = 0.973\ (\text{Reading}_{\text{instrument}}) - 8.6843, \quad r^2 = 0.998 \qquad (1)$$

B.2. Paint Booth Freestream Velocity Profile

The paint booth is located in the basement of the Rosenau Hall on the campus of the Univeristy of North Carolina at Chapel Hill. A twelve point traverse was performed at across the paint booth cross section. The room housing the paint spray booth was in the machine shop of the School of Public Health with several benches and cabinets located

near the inlet to the booth which caused fairly high turbulence in the paint booth. A layout of the paint booth and machine shop is shown in Figure B.2. A bank of filters were installed in the rear of the booth to collect the overspray and assist in maintaining uniform airstream velocity throughout the booth. A sheet metal flange was also installed on the entrance to the booth to minimize the effects of flow separation at the booth entrance. The flowrate through the tunnel is adjustable by varying a pulley on the fan belts which in turn causes the fan blades to spin at higher/lower revolutions per minute (rpm). The fan was set initially to approximately 100 fpm and was not varied during the experiment due to difficulty in precise adjustment of fan speed. The air velocity was measured by the thermo-anemometer on a 12 point grid across a the paint booth cross section and the results are shown in Table B.2.

B.3. Experimental Setup

The setup of the HVLP spraygun and pot was identical to that described in appendix A section A.6. A schematic of the HVLP spray painting setup is shown in Figure A.6. The liquid and air adjustment screws were set to the same positions as used in the wind tunnel tests. A compressor provided the air for the spray gun and the operation was identical to that described previously for the experimental wind tunnel operation.

B.4. Filter and Vacuum Oil Weights

The PVC 37 mm sampling filters were placed in a desiccator for a period of at least 2 hours prior to and following sampling. The filters were weighed on a Cahn 27 Electrobalance on the 20 Loop A setting which has a range of 0-20 mg with a resolution of 1μg. The sensitivity of the balance is reported to be 0.0001 mg with an accuracy of ±0.005%. The balance was zeroed and calibrated with a 200 mg Class M calibrating weight in accordance with manufacturer's specifications before each series of experimental runs. A radioactive ionizing unit was passed over the filters before weighing to discharge any static electricity buildup on the filter which may cause erroneous readings.

The mass of liquid used during the experimental runs and the mass transferred to the plate was measured by a mass balance method. The liquid feed pot was weighed prior to each run and following the completion of each run. The amount of liquid transferred was measured by the weighing of the drip trough placed underneath the plate before and after each run. An Ohaus Model 1900 Industrial Lab Balance was used to measure the quanities of liquid used and transferred.

B.5. Experimental Data

The experimental identification table is shown in Table B.2. This table shows the conditions under which the test run was performed including data such as environmental conditions, freestream velocity (U), mannequin orientation, nozzle pressure (p_n) breathing

zone concentration (BZC) sample location, and dimensionless nozzle pressure (Carlton number). Breathing zone concentration samples were collected nly on the downstream lapel for each run during the paint booth runs. The calculated overspray data is shown in Table B.3. This table includes information such as mass flow rates of air and liquid, mass of liquid transferred, and overspray generation rate (m_0), and transfer efficiency. The breathing zone concentration data is shown in Table B.4. This table includes information such as sample filter weights, blank filter weights, and calculated dimensionless concentration. Sample calculations are shown in section A.11.

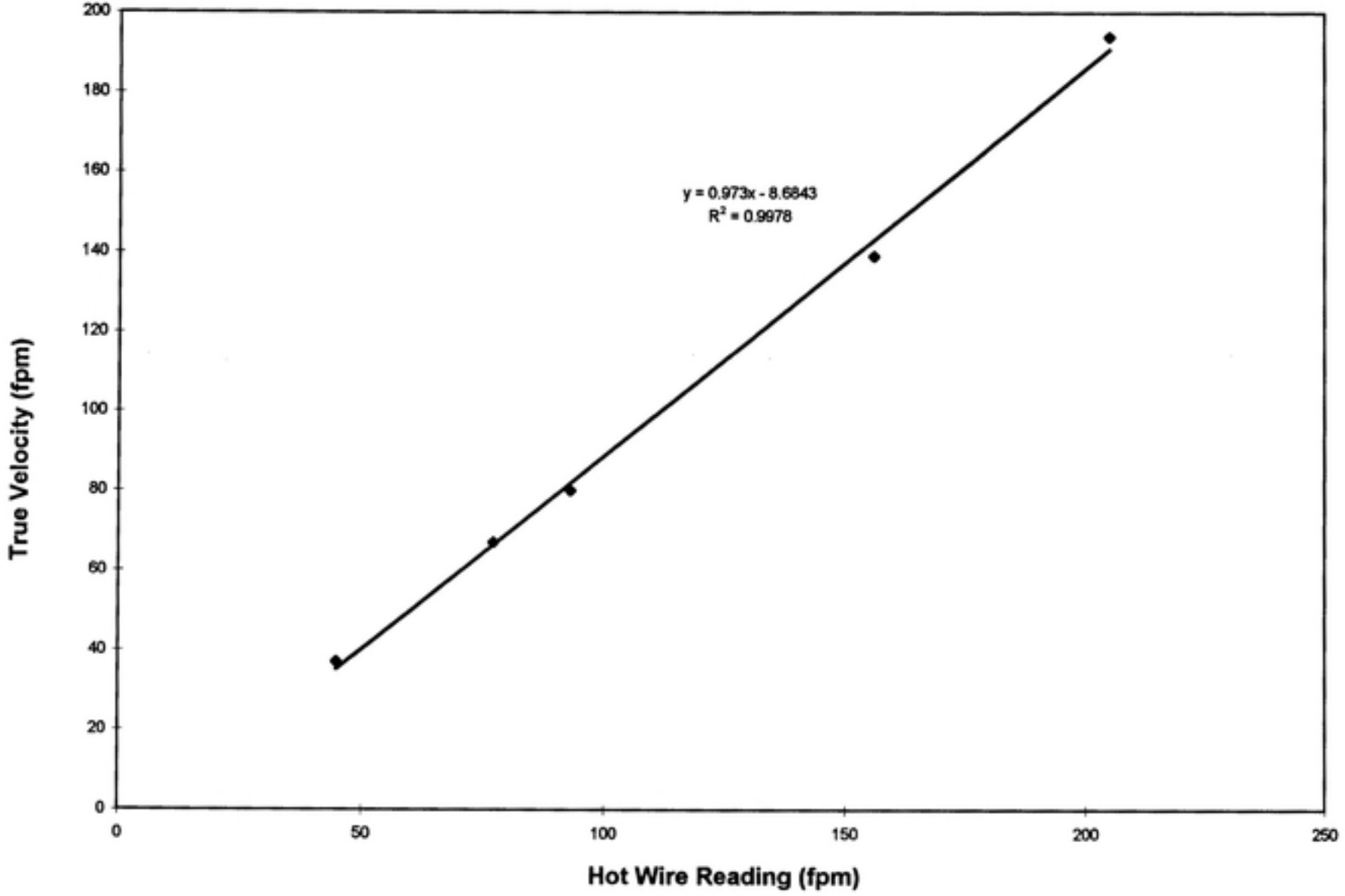

Figure B.1: Thermo-Anemometer Calibration Curve

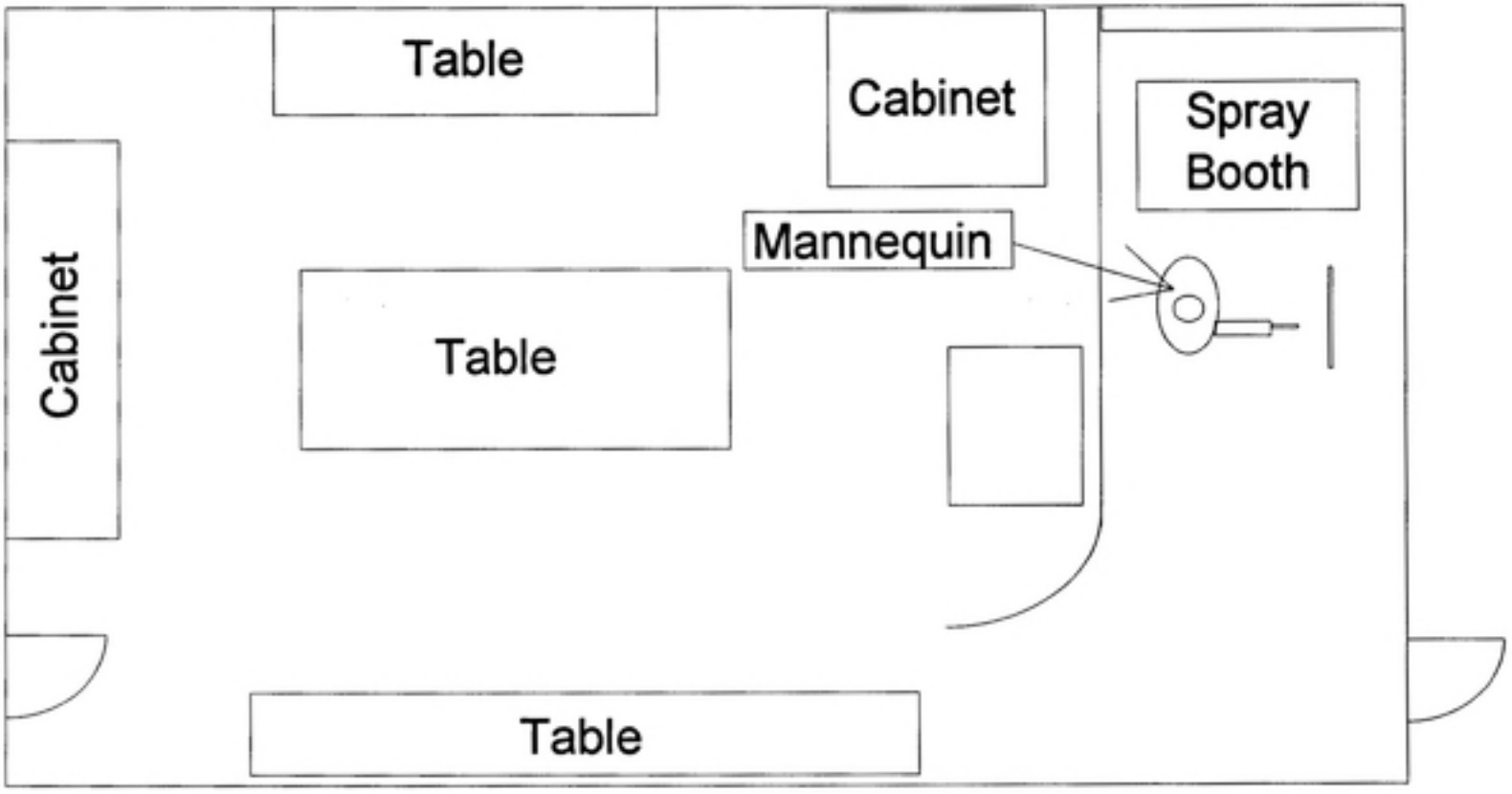

Figure B.2: Paint Booth Area Layout

Table B.1.: Thermo-Anemometer Calibration Data

Orifice Pressure (in wg)	SQRT (Orifice Pressure (in wg)	Velocity in Duct (fpm)	Air Volume (Q), CFM	Velocity in Small Wind Tunnel (fpm)	Direct Reading Thermal Anemometer (fpm)
0.08	0.28	1080	94	37	45
0.30	0.55	1951	170	67	77
0.41	0.64	2326	203	80	93
1.30	1.14	4047	353	139	156
2.30	1.52	5657	494	194	205

Table B.2: Paint Booth Velocity Profile

44.5	91.4	120.5
52.3	99.3	129.4
102.1	96.4	145.7
119.3	115.4	138.8

Note: All Velocities are in feet per minute (fpm).

Table B.3: Experimental Identifier Sheet

Run Number	Static Pressure (in wg)	Freestream Velocity (fpm)	Liquid Temperature (F)	Viscosity (cp)	Air Temperature (F)	Gauge Pressure (psig)	Nozzle Pressure Cap (psig)	Nozzle Pressure Cap&Horn (psig)	Orientation	Sample Location
1	n/a	93.0	74	70.54	74	53	6.5	11.5	90°	Upstream
2	n/a	93.0	74	70.54	74	46	6	10.5	90°	Downstream
3	n/a	93.0	74	70.54	74	27	2.5	4.5	90°	Upstream
4	n/a	93.0	74	70.54	74	16	1.5	2.5	90°	Downstream
Blank	n/a	n/a	n/a	n/a	n/a	n/a	n/a	n/a	n/a	n/a
5	n/a	93.0	73	72.73	75	53	6.5	11.5	90°	Upstream
6	n/a	93.0	73	72.73	75	46	6	10.5	90°	Downstream
7	n/a	93.0	73	72.73	75	27	2.5	4.5	90°	Upstream
Blank	n/a	n/a	n/a	n/a	n/a	n/a	n/a	n/a	n/a	n/a
8	n/a	93.0	72	74.99	75	27	2.5	4.5	90°	Upstream
9	n/a	93.0	72	74.99	75	46	6	10.5	90°	Downstream
10	n/a	93.0	72	74.99	75	53	6.5	11.5	90°	Upstream
Blank	n/a	n/a	n/a	n/a	n/a	n/a	n/a	n/a	n/a	n/a

Table B.4:Transfer Efficiency/Overspray Worksheet

Run Number	Run Time (s)	Bucket Weight (g)		Trough Weight (g)		Mass of Liquid Sprayed (g/min)	Mass of Liquid Transferred (g/min)	Mass of Liquid Overspray (m_o) (g/min)	Mass of Air (g/min)**	m_o/m_t	Transfer Efficiency	Carlton Number
		Before	After	Before	After							
1	242.45	3109.8	2538.3	234.8	692.5	141.4	113.3	28.2	285	2.0	0.801	1.8E+6
2	301.91	2977.7	2257.5	243	828.3	143.1	116.3	26.8	268	1.9	0.813	1.6E+6
3	570.87	2840.5	1556.7	244.5	1357.6	134.9	117.0	17.9	165	1.2	0.867	6.8E+5
4	781.6	2663.2	974.5	251.3	1756.5	129.6	115.5	14.1	131	1.0	0.891	4.1E+5
Blank	n/a	n/a	n/a	n/a	n/a	n/a	n/a	n/a	n/a	n/a	n/a	n/a
5	240.92	3383.8	2848.4	236.5	655.6	133.3	104.4	29.0	285	2.1	0.783	1.7E+6
6	304.97	3250.5	2565.3	251.6	805.8	134.8	109.0	25.8	268	2.0	0.809	1.6E+6
7	571.87	3120.5	1880.3	250.3	1322.5	130.1	112.5	17.6	165	1.3	0.865	6.6E+5
Blank	n/a	n/a	n/a	n/a	n/a	n/a	n/a	n/a	n/a	n/a	n/a	n/a
8	660.89	3460	2192	244.8	1329.5	115.1	98.5	16.6	165	1.4	0.855	6.4E+5
9	300.8	3283.5	2667.3	238.1	732.3	122.9	98.6	24.3	268	2.2	0.802	1.5E+6
10	243.2	3157	2649.6	239.8	636.5	125.2	97.9	27.3	285	2.3	0.782	1.7E+6
Blank	n/a	n/a	n/a	n/a	n/a	n/a	n/a	n/a	n/a	n/a	n/a	n/a

Table B.5: Dimensionless Concentration Worksheet

Run Number	Date	Mass of Liquid Overspray (m_o) (g/min)	Time (s)	Filter Weight (m)		Sample Mass (mg)	Sampling Flowrate (lpm)	Concentration (mg/m³)	Carlton Number	CUHD/m_o
				Before	After					
1	12/13/96	28.16	242.45	14.419	15.684	1.265	1.90	165.20	1.6E+6	0.0768
2	12/13/96	26.81	301.91	14.241	15.572	1.331	1.90	139.59	1.8E+6	0.0682
3	12/13/96	17.94	570.87	14.362	14.783	0.421	1.90	23.35	6.8E+5	0.0170
4	12/13/96	14.09	781.6	13.889	13.880	-0.009	1.90	-0.36	4.1E+5	-0.0003
Blank	12/13/96	n/a	n/a	13.432	13.433	0.001	n/a	n/a	n/a	n/a
5	12/14/96	28.96	240.92	13.199	14.376	1.177	1.90	154.68	1.6E+6	0.0699
6	12/14/96	25.77	304.97	13.669	14.892	1.223	1.90	126.97	1.7E+6	0.0645
7	12/14/96	17.63	571.87	13.680	13.858	0.178	1.90	9.86	6.6E+5	0.0073
Blank	12/14/96	n/a	n/a	13.433	13.430	-0.003	n/a	n/a	n/a	n/a
8	12/15/96	16.64	660.89	13.577	13.840	0.263	1.91	12.51	1.5E+6	0.0098
9	12/15/96	24.34	300.8	13.351	14.450	1.099	1.91	114.89	6.4E+5	0.0618
10	12/15/96	27.31	243.2	13.299	14.375	1.076	1.91	139.13	1.7E+6	0.0667
Blank	12/15/96	n/a	n/a	13.430	13.431	0.001	n/a	n/a	n/a	n/a

Appendix C: Statistical Analysis and Results

C.1. Wind Tunnel Blockage Partial F Test

A test of coincidence was performed for the wind tunnel and paint booth data sets. This test uses a single multiple regression model that contains dummy variables to account for each group. An analysis using the SAS system was performed and the variable names used in the model are as follows:

1) Dummy Variable: ENC stands for enclosure and is either coded as p for paint booth or w for wind tunnel.

2) Dependent Variable: DC stands for dimensionless concentration, $\frac{CHUD}{m_0}$

3) Independent Variable: CN stands for Carlton number, $\frac{p_a H}{\mu_t U}$

The hypothesis is that the two regression lines were coincident (i.e. the slopes and intercepts were equal). The two models being compared in this test are therefore:

Full Model: $DC = \beta_0 + \beta_1 CN + \beta_2 ENC + \beta_3 (CN)(ENC) + E$

Reduced Model: $DC = \beta_0 + \beta_1 CN + E$

Test statistic: $$F = \frac{[\text{regression SS (CN, ENC, CN*ENC)} - \text{regression SS (CN)}]}{\text{MS residual (CN, ENC, CN*ENC)}}$$

$$F = \frac{[0.01853125 - 0.01796297]/2}{[0.02125171/20]} = 0.2674$$

Comparing this F with $F_{2, 20, 0.95} = 3.49$, we accept the null hypothesis at a level of significance $\alpha = 0.05$ and conclude that there is strong evidence that the two lines are coincident. Therefore, we can conclude that there is no significant difference between the wind tunnel and paint booth data sets. The SAS program output is shown in Figure C.1.

Figure C.1: SAS Output

Method I

General Linear Models Procedure

Dependent Variable: DC

Source	DF	Sum of Squares	Mean Square	F Value	Pr > F
Model	3	0.01853125	0.00617708	38.60	0.0001
Error	17	0.00272047	0.00016003		
Corrected Total	20	0.02125171			

R-Square	C.V.	Root MSE	DC Mean
0.871988	24.86448	0.01265020	0.05087657

Source	DF	Type I SS	Mean Square	F Value	Pr > F
CN	1	0.01796297	0.01796297	112.25	0.0001
ENC	1	0.00024853	0.00024853	1.55	0.2296
CN*ENC	1	0.00031974	0.00031974	2.00	0.1756

Source	DF	Type III SS	Mean Square	F Value	Pr > F
CN	1	0.01491359	0.01491359	93.19	0.0001
ENC	1	0.00051123	0.00051123	3.19	0.0917
CN*ENC	1	0.00031974	0.00031974	2.00	0.1756

Parameter		Estimate	T for H0: Parameter=0	Pr > |T|	Std Error of Estimate
INTERCEPT		0.0005342564 B	0.08	0.9397	0.00696221
CN		0.0000000421 B	8.72	0.0001	0.00000000
ENC	p	-.0256441624 B	-1.79	0.0917	0.01434759
	w	0.0000000000 B	.	.	.
CN*ENC	p	0.0000000144 B	1.41	0.1756	0.00000001
	w	0.0000000000 B	.	.	.

NOTE: The X'X matrix has been found to be singular and a generalized inverse was used to solve the normal equations.
Estimates followed by the letter 'B' are biased, and are not unique estimators of the parameters.